



Bearing Capacity of Soils II

Course Number: GE-02-302

PDH: 3

Approved for: AK, AL, AR, GA, IA, IL, IN, KS, KY, LA, MD, ME, MI, MN, MO, MS, MT, NC, ND, NE, NH, NJ, NM, NV, OH, OK, OR, PA, SC, SD, TN, TX, UT, VA, VT, WI, WV, and WY

New Jersey Professional Competency Approval #24GP00025600

North Carolina Approved Sponsor #S-0695

Maryland Approved Provider of Continuing Professional Competency

Indiana Continuing Education Provider #CE21800088

This document is the course text. You may review this material at your leisure before or after you purchase the course. In order to obtain credit for this course, complete the following steps:

1) Log in to My Account and purchase the course. If you don't have an account, go to New User to create an account.

2) After the course has been purchased, review the technical material and then complete the quiz at your convenience.

3) A Certificate of Completion is available once you pass the exam (70% or greater). If a passing grade is not obtained, you may take the quiz as many times as necessary until a passing grade is obtained (up to one year from the purchase date).

If you have any questions or technical difficulties, please call (508) 298-4787 or email us at admin@PDH-Pro.com.



CECW-EG Engineer Manual 1110-1-1905	Department of the Army U.S. Army Corps of Engineers Washington, DC 20314-1000	EM 1110-1-1905
	Engineering and Design BEARING CAPACITY OF SOILS	
	Distribution Restriction Statement Approved for public release; distribution is unlimited.	

CHAPTER 5

DEEP FOUNDATIONS

5-1. **Basic Considerations.** Deep foundations transfer loads from structures to acceptable bearing strata at some distance below the ground surface. These foundations are used when the required bearing capacity of shallow foundations cannot be obtained, settlement of shallow foundations is excessive, and shallow foundations are not economical. Deep foundations are also used to anchor structures against uplift forces and to assist in resisting lateral and overturning forces. Deep foundations may also be required for special situations such as expansive or collapsible soil and soil subject to erosion or scour.

a. **Description.** Bearing capacity analyses are performed to determine the diameter or cross-section, length, and number of drilled shafts or driven piles required to support the structure.

(1) **Drilled Shafts.** Drilled shafts are nondisplacement reinforced concrete deep foundation elements constructed in dry, cased, or slurry-filled boreholes. A properly constructed drilled shaft will not cause any heave or loss of ground near the shaft and will minimize vibration and soil disturbance. Dry holes may often be bored within 30 minutes leading to a rapidly constructed, economical foundation. Single drilled shafts may be built with large diameters and can extend to deep depths to support large loads. Analysis of the bearing capacity of drilled shafts is given in Section I.

(a) Lateral expansion and rebound of adjacent soil into the bored hole may decrease pore pressures. Heavily overconsolidated clays and shales may weaken and transfer some load to the shaft base where pore pressures may be positive. Methods presented in Section I for calculating bearing capacity in clays may be slightly unconservative, but the FS's should provide an adequate margin of safety against overload.

(b) Rebound of soil at the bottom of the excavation and water collecting at the bottom of an open bore hole may reduce end bearing capacity and may require construction using slurry.

(c) Drilled shafts tend to be preferred to driven piles as the soil becomes harder, pile driving becomes difficult, and driving vibrations affect nearby structures. Good information concerning rock is required when drilled shafts are carried to rock. Rock that is more weathered or of lesser quality than expected may require shaft bases to be placed deeper than expected. Cost overruns can be significant unless good information is available.

(2) **Driven Piles.** Driven piles are displacement deep foundation elements driven into the ground causing the soil to be displaced and disturbed or remolded. Driving often temporarily increases pore pressures and reduces short term bearing capacity, but may increase long term bearing capacity. Driven piles are often constructed in groups to provide adequate bearing capacity. Analysis of the bearing capacity of driven piles and groups of driven piles is given in Section II.

(a) Driven piles are frequently used to support hydraulic structures such as locks and retaining walls and to support bridges and highway overpasses. Piles are also useful in flood areas with unreliable soils.

(b) Pile driving causes vibration with considerable noise and may interfere with the performance of nearby structures and operations. A preconstruction survey of nearby structures may be required.

(c) The cross-section and length of individual piles are restricted by the capacity of equipment to drive piles into the ground.

(d) Driven piles tend to densify cohesionless soils and may cause settlement of the surface, particularly if the soil is loose.

(e) Heave may occur at the surface when piles are driven into clay, but a net settlement may occur over the longterm. Soil heave will be greater in the direction toward which piles are placed and driven. The lateral extent of ground heave is approximately equal to the depth of the bottom of the clay layer.

(3) **Structural capacity.** Stresses applied to deep foundations during driving or by structural loads should be compared with the allowable stresses of materials carrying the load.

b. **Design Responsibility.** Selection of appropriate design and construction methods requires geotechnical and structural engineering skills. Knowledge of how a deep foundation interacts with the superstructure is provided by the structural engineer with soil response information provided by the geotechnical engineer. Useful soil-structure interaction analyses can then be performed of the pile-soil support system.

c. **Load Conditions.** Mechanisms of load transfer from the deep foundation to the soil are not well understood and complicate the analysis of deep foundations. Methods available and presented below for evaluating ultimate bearing capacity are approximate. Consequently, load tests are routinely performed for most projects, large or small, to determine actual bearing capacity and to evaluate performance. Load tests are not usually performed on drilled shafts carried to bedrock because of the large required loads and high cost.

(1) **Representation of Loads.** The applied loads may be separated into vertical and horizontal components that can be evaluated by soil-structure interaction analyses and computer-aided methods. Deep foundations must be designed and constructed to resist both applied vertical and lateral loads, Figure 5-1. The applied vertical load Q is supported by soil-shaft side friction Q_{su} and base resistance Q_{bu} . The applied lateral load T is carried by the adjacent lateral soil and structural resistance of the pile or drilled shaft in bending, Figure 5-2.

(a) Applied loads should be sufficiently less than the ultimate bearing capacity to avoid excessive vertical and lateral displacements of the pile or drilled shaft. Displacements should be limited to 1 inch or less.

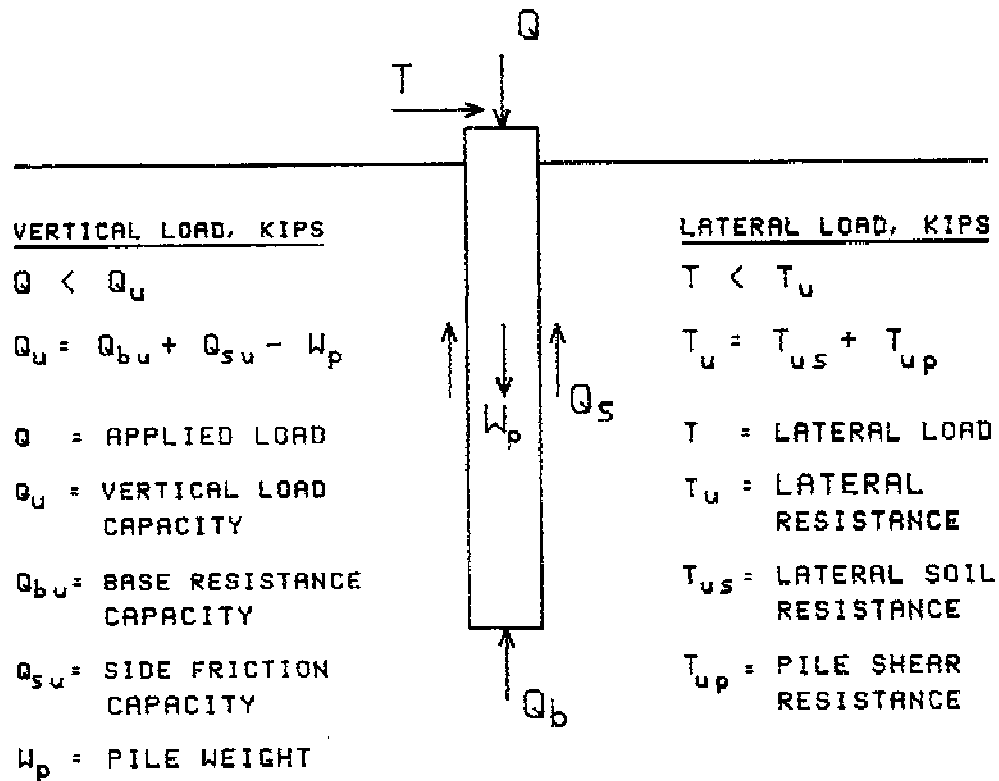


Figure 5-1. Support of deep foundations

(b) Factors of safety applied to the ultimate bearing capacity to obtain allowable loads are often 2 to 4. FS applied to estimations of the ultimate bearing capacity from static load test results should be 2.0. Otherwise, FS should be at least 3.0 for deep foundations in both clay and sand. FS should be 4 for deep foundations in multi-layer clay soils and clay with undrained shear strength $C_u > 6$ ksf.

(2) **Side Friction.** Development of soil-shaft side friction resisting vertical loads leads to relative movements between the soil and shaft. The maximum side friction is often developed after relative small displacements less than 0.5 inch. Side friction is limited by the adhesion between the shaft and the soil or else the shear strength of the adjacent soil, whichever is smaller.

(a) Side friction often contributes the most bearing capacity in practical situations unless the base is bearing on stiff shale or rock that is much stiffer and stronger than the overlying soil.

(b) Side friction is hard to accurately estimate, especially for foundations constructed in augered or partially jetted holes or foundations in stiff, fissured clays.

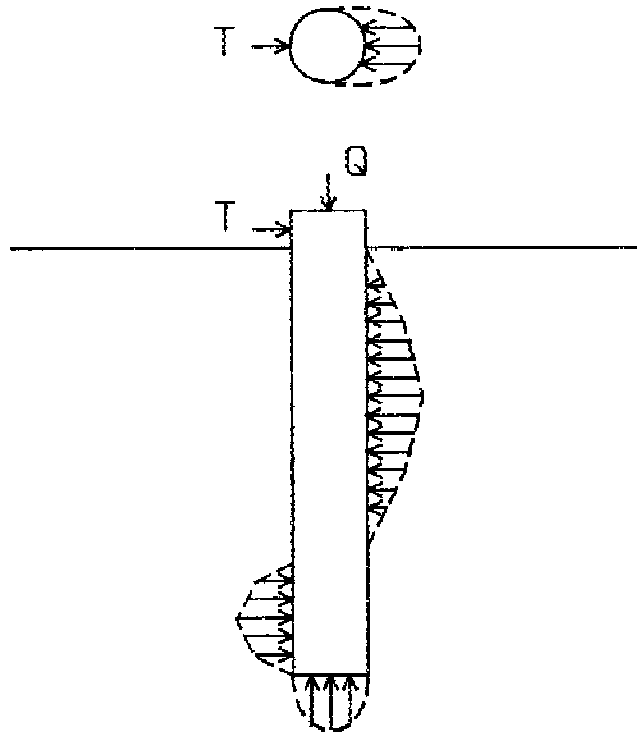


Figure 5-2. Earth pressure distribution T_{us} acting on a laterally loaded pile

(3) **Base Resistance.** Failure in end bearing normally consists of a punching shear at the tip. Applied vertical compressive loads may also lead to several inches of compression prior to a complete plunging failure. The full soil shear strength may not be mobilized beneath the pile tip and a well-defined failure load may not be observed when compression is significant.

Section I. Drilled Shafts

5-2. **Vertical Compressive Capacity of Single Shafts.** The approximate static load capacity of single drilled shafts from vertical applied compressive forces is

$$Q_u \approx Q_{bu} + Q_{su} - W_p \quad (5-1a)$$

$$Q_u \approx q_{bu}A_b + \sum_{i=1}^n Q_{sui} - W_p \quad (5-1b)$$

where

- Q_u = ultimate drilled shaft or pile resistance, kips
- Q_{bu} = ultimate end bearing resistance, kips
- Q_{su} = ultimate skin friction, kips
- q_{bu} = unit ultimate end bearing resistance, ksf
- A_b = area of tip or base, ft^2
- n = number of increments the pile is divided for analysis (referred to as a pile element, Figure C-1)

Q_{sui} = ultimate skin friction of pile element i , kips
 W_p = pile weight, $\approx A_b \cdot L \cdot \gamma_p$ without enlarged base, kips
 L = pile length, ft
 γ_p = pile density, kips/ft³

A pile may be visualized to consist of a number of elements as illustrated in Figure C-1, Appendix C, for the calculation of ultimate bearing capacity.

a. **End Bearing Capacity.** Ultimate end bearing resistance at the tip may be given as Equation 4-1 neglecting pile weight W_p

$$Q_{bu} = c \cdot N_{cp} \cdot \zeta_{cp} + \sigma'_L \cdot N_{qp} \cdot \zeta_{qp} + \frac{B_b}{2} \cdot \gamma'_b \cdot N_{\gamma p} \cdot \zeta_{\gamma p} \quad (5-2a)$$

where

c = cohesion of soil beneath the tip, ksf
 σ'_L = effective soil vertical overburden pressure at pile base $\approx \gamma'_L \cdot L$, ksf
 γ'_L = effective wet unit weight of soil along shaft length L , kips/ft³
 B_b = base diameter, ft
 γ'_b = effective wet unit weight of soil in failure zone beneath base, kips/ft³
 $N_{cp}, N_{qp}, N_{\gamma p}$ = pile bearing capacity factors of cohesion, surcharge, and wedge components
 $\zeta_{cp}, \zeta_{qp}, \zeta_{\gamma p}$ = pile soil and geometry correction factors of cohesion, surcharge, and wedge components

Methods for estimating end bearing capacity and correction factors of Equation 5-2a should consider that the bearing capacity reaches a limiting constant value after reaching a certain critical depth. Methods for estimating end bearing capacity from in situ tests are discussed in Section II on driven piles.

(1) **Critical Depth.** The effective vertical stress appears to become constant after some limiting or critical depth L_c , perhaps from arching of soil adjacent to the shaft length. The critical depth ratio L_c/B where B is the shaft diameter may be found from Figure 5-3. The critical depth applies to the Meyerhof and Nordlund methods for analysis of bearing capacity.

(2) **Straight Shafts.** Equation 5-2a may be simplified for deep foundations without enlarged tips by eliminating the $N_{\gamma p}$ term

$$Q_{bu} = c \cdot N_{cp} \cdot \zeta_{cp} + \sigma'_L \cdot (N_{qp} - 1) \cdot \zeta_{qp} \quad (5-2b)$$

or

$$Q_{bu} = c \cdot N_{cp} \cdot \zeta_{cp} + \sigma'_L \cdot N_{qp} \cdot \zeta_{qp} \quad (5-2c)$$

Equations 5-2b and 5-2c also compensates for pile weight W_p assuming $\gamma_p \approx \gamma'_L$. Equation 5-2c is usually used rather than Equation 5-2b because N_{qp} is usually large compared with "1" and $N_{qp} - 1 \approx N_{qp}$. W_p in Equation 5-1 may be ignored when calculating Q_u .

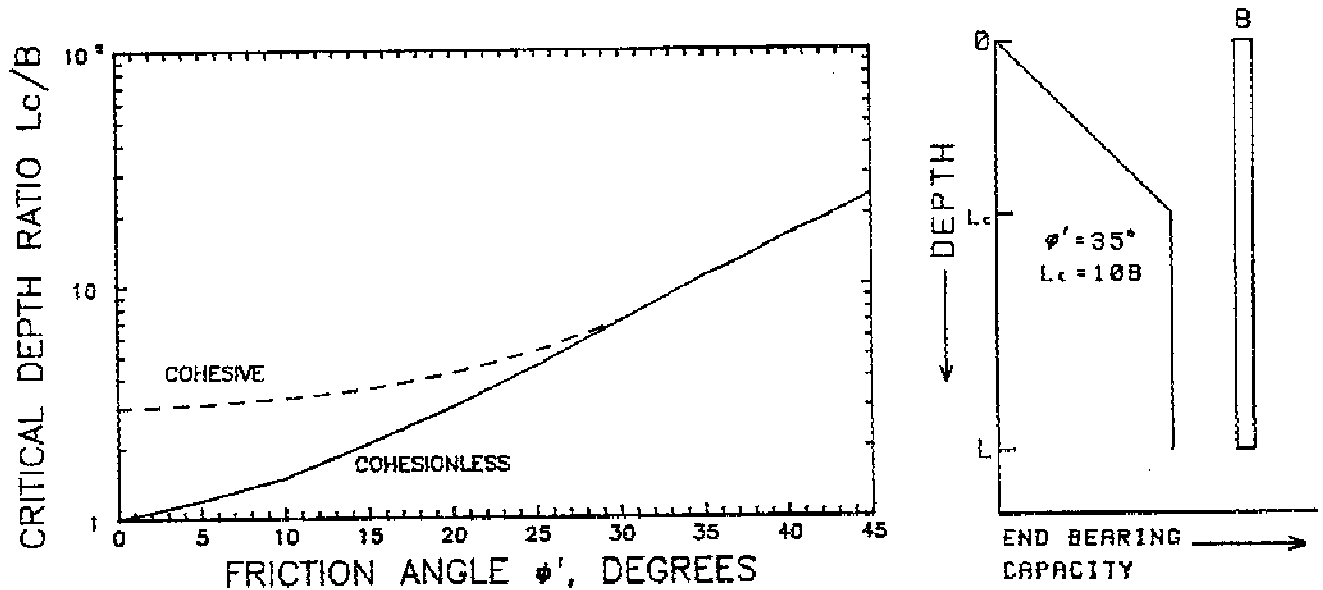


Figure 5-3. Critical depth ratio L_c/B (Data from Meyerhof 1976)

(3) **Cohesive Soil.** The undrained shear strength of saturated cohesive soil for deep foundations in saturated clay subjected to a rapidly applied load is $c = C_u$ and the friction angle $\phi = 0$. Equations 5-2 simplifies to (Reese and O'Neill 1988)

$$q_{bu} = F_r N_{cp} C_u, \quad q_{bu} \leq 80 \text{ksf} \quad (5-3)$$

where the shape factor $\zeta_{cp} = 1$ and $N_{cp} = 6 \cdot [1 + 0.2 \cdot (L/B_b)] \leq 9$. The limiting q_{bu} of 80 ksf is the largest value that has so far been measured for clays. C_u may be reduced by about 1/3 in cases where the clay at the base has been softened and could cause local high strain bearing failure. F_r should be 1.0, except when B_b exceeds about 6 ft. For base diameter $B_b > 6$ ft,

$$F_r = \frac{2.5}{aB_b + 2.5b}, \quad F_r \leq 1.0 \quad (5-4)$$

where

$$a = 0.0852 + 0.0252(L/B_b), \quad a \leq 0.18$$

$$b = 0.45C_u^{0.5}, \quad 0.5 \leq b \leq 1.5$$

The undrained strength of soil beneath the base C_u is in units of ksf. Equation 5-3 limits q_{bu} to bearing pressures for a base settlement of 2.5 inches. The undrained shear strength C_u is estimated by methods in Chapter 3 and may be taken as the average shear strength within $2B_b$ beneath the tip of the shaft.

(4) **Cohesionless Soil.** Hanson, Vesic, Vesic Alternate, and general shear methods of estimating the bearing capacity and adjustment factors are recommended for solution of ultimate end bearing capacity using Equations 5-2. The Vesic method requires volumetric strain data ϵ_v of the foundation soil in addition to the

effective friction angle ϕ' . The Vesic Alternate method provides a lower bound estimate of bearing capacity. The Alternate method may be more appropriate for deep foundations constructed under difficult conditions, for drilled shafts placed in soil subject to disturbance and when a bentonite-water slurry is used to keep the hole open during drilled shaft construction. Several of these methods should be used for each design problem to provide a reasonable range of the probable bearing capacity if calculations indicate a significant difference between methods.

(a) Hanson Method. The bearing capacity factors N_{cp} , N_{qp} , and N_{yp} and correction factors ζ_{cp} , ζ_{qp} , and ζ_{yp} for shape and depth from Table 4-5 may be used to evaluate end bearing capacity using Equations 5-2. Depth factors ζ_{cd} and ζ_{qd} contain a "k" term that prevents unlimited increase in bearing capacity with depth. $k = \tan^{-1}(L_b/B)$ in radians where L_b is the embedment depth in bearing soil and B is the shaft diameter. $L_b/B \leq L_c/B$, Figure 5-3.

(b) Vesic Method. The bearing capacity factors of Equation 5-2b are estimated by (Vesic 1977)

$$N_{cp} = (N_{qp} - 1) \cdot \cot \phi' \quad (5-5a)$$

$$N_{qp} = \frac{3}{3 - \sin \phi} \cdot e^{\frac{(90 - \phi') \pi \tan \phi}{180}} \cdot \tan^2 \left[45 + \frac{\phi'}{2} \right] \cdot I_{rr}^{\frac{4 \sin \phi'}{3(1 + \sin \phi)}} \quad (5-5b)$$

$$I_{rr} = \frac{I_r}{1 + \epsilon_v \cdot I_r} \quad (5-5c)$$

$$I_r = \frac{G_s}{c + \sigma'_r \tan \phi'} \quad (5-5d)$$

$$\epsilon_v = \frac{1 - 2v_s}{2(1 - v_s)} \cdot \frac{\sigma'_L}{G_s} \quad (5-5e)$$

where

- I_{rr} = reduced rigidity index
- I_r = rigidity index
- ϵ_v = volumetric strain, fraction
- v_s = soil Poisson's ratio
- G_s = soil shear modulus, ksf
- c = undrained shear strength C_u , ksf
- ϕ' = effective friction angle, deg
- σ'_L = effective soil vertical overburden pressure at pile base, ksf

$I_{rr} \approx I_r$ for undrained or dense soil where $v_s \approx 0.5$. G_s may be estimated from laboratory or field test data, Chapter 3, or by methods described in EM 1110-1-1904. The shape factor $\zeta_{cp} = 1.00$ and

$$\zeta_{qp} = \frac{1 + 2K_o}{3} \quad (5-6a)$$

$$K_o = (1 - \sin \phi') \cdot OCR^{\sin \phi'} \quad (5-6b)$$

where

K_o = coefficient of earth pressure at rest
OCR = overconsolidation ratio

The OCR can be estimated by methods described in Chapter 3 or EM 1110-1-1904. If the OCR is not known, the Jaky equation can be used

$$K_o = 1 - \sin \phi' \quad (5-6c)$$

(c) Vesic Alternate Method. A conservative estimate of N_{qp} can be readily made by knowing only the value of ϕ'

$$N_{qp} = (1 + \tan \phi') \cdot e^{\tan \phi'} \cdot \tan^2 \left[45 + \frac{\phi'}{2} \right] \quad (5-7)$$

The shape factor ζ_{qp} may be estimated by Equations 5-6. Equation 5-7 assumes a local shear failure and hence leads to a lower bound estimate of q_{bu} . A local shear failure can occur in poor soils such as loose silty sands or weak clays or else in soils subject to disturbance.

(d) General Shear Method. The bearing capacity factors of Equation 5-2b may be estimated assuming general shear failure by (Bowles 1968)

$$N_{qp} = \frac{e^{\frac{270 - \phi'}{180} \cdot \pi \cdot \tan \phi'}}{2 \cdot \cos^2 \left[45 + \frac{\phi'}{2} \right]} \quad (5-8)$$

The shape factor $\zeta_{qp} = 1.00$. $N_{cp} = (N_{qp} - 1) \cot \phi'$.

b. **Skin Friction Capacity.** The maximum skin friction that may be mobilized along an element of shaft length ΔL may be estimated by

$$Q_{sui} = A_{si} \cdot f_{si} \quad (5-9)$$

where

A_{si} = surface area of element i , $C_{si} \cdot \Delta L$, ft^2
 C_{si} = shaft circumference at element i , ft
 ΔL = length of pile element, ft
 f_{si} = skin friction at pile element i , ksf

Resistance to applied loads from skin friction along the shaft perimeter increases with increasing depth to a maximum, then decreases toward the tip. One possible distribution of skin friction is indicated in Figure 5-4. The estimates of skin friction f_{si} with depth is at best approximate. Several methods of estimating f_{si} , based on past experience and the results of load tests, are described below. The vertical load on the shaft may initially increase slightly with increasing depth near the ground surface because the pile adds weight which may not be supported by the small skin friction near the surface. Several of these methods should be used when possible to provide a range of probable skin friction values.

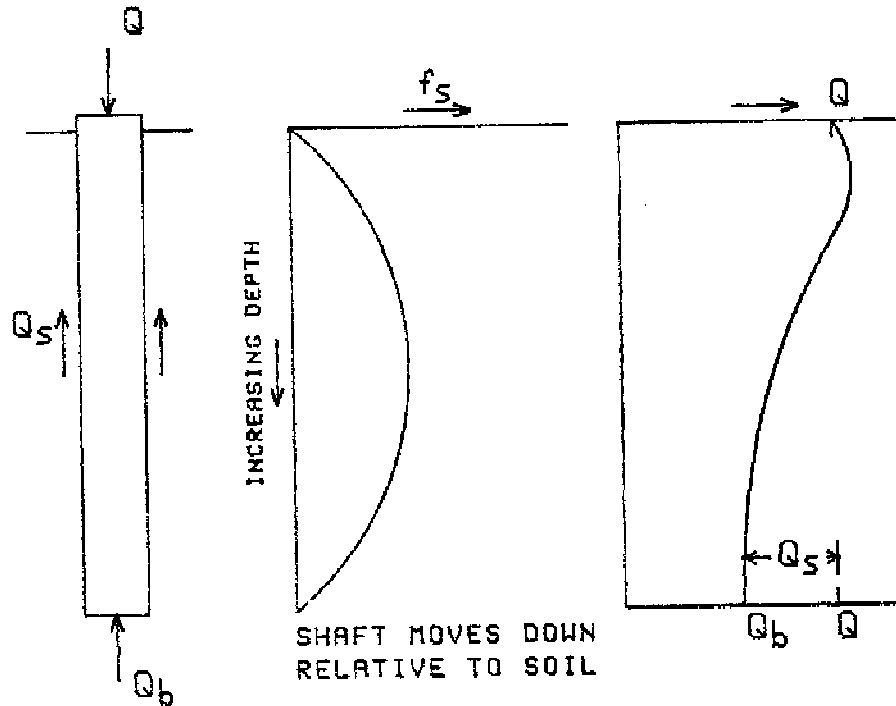


Figure 5-4. An example distribution of skin friction in a pile

(1) **Cohesive Soil.** Adhesion of cohesive soil to the shaft perimeter and the friction resisting applied loads are influenced by the soil shear strength, soil disturbance and changes in pore pressure, and lateral earth pressure existing after installation of the deep foundation. The average undrained shear strength determined from the methods described in Chapter 3 should be used to estimate skin friction. The friction angle ϕ is usually taken as zero.

(a) The soil-shaft skin friction f_{si} of a length of shaft element may be estimated by

$$f_{si} = \alpha_a \cdot C_u \quad (5-10)$$

where

α_a = adhesion factor
 C_u = undrained shear strength, ksf

Local experience with existing soils and load test results should be used to estimate appropriate α_a . Estimates of α_a may be made from Table 5-1 in the absence of load test data and for preliminary design.

TABLE 5-1

Adhesion Factors for Drilled Shafts in a Cohesive Soil
(Reese and O'Neill 1988)

Shaft Depth, ft	Adhesion Factor α_a
0 - 5	0.0
Shaft diameter from bottom of straight shaft or from top of underream	0.0
All Other Points	0.55

Note: skin friction f_{si} should be limited to 5.5 ksf

STRAIGHT SHAFT

UNDERREAMED SHAFT

(b) The adhesion factor may also be related to the plasticity index PI for drilled shafts constructed dry by (Data from Stewart and Kulhawy 1981)

Overconsolidated: $\alpha_a = 0.7 - 0.01 \cdot PI$ (5-11a)

Slightly over-consolidated (OCR ≤ 2): $\alpha_a = 0.9 - 0.01 \cdot PI$ (5-11b)

Normally consolidated: $\alpha_a = 0.9 - 0.004 \cdot PI$ (5-11c)

where $15 < PI < 80$. Drilled shafts constructed using the bentonite-water slurry should use α_a of about 1/2 to 2/3 of those given by Equations 5-11.

(2) **Cohesionless Soil.** The soil-shaft skin friction may be estimated using effective stresses with the beta method

$$f_{si} = \beta_f \cdot \sigma'_i \quad (5-12a)$$

$$\beta_f = K \cdot \tan \delta_a \quad (5-12b)$$

where

β_f = lateral earth pressure and friction angle factor

K = lateral earth pressure coefficient

δ_a = soil-shaft effective friction angle, $\leq \phi'$, degrees

σ'_i = effective vertical stress in soil in shaft (pile) element i , ksf

The cohesion c is taken as zero.

(a) Figure 5-5 indicates appropriate values of β_f as a function of the effective friction angle ϕ' of the soil prior to installation of the deep foundation.

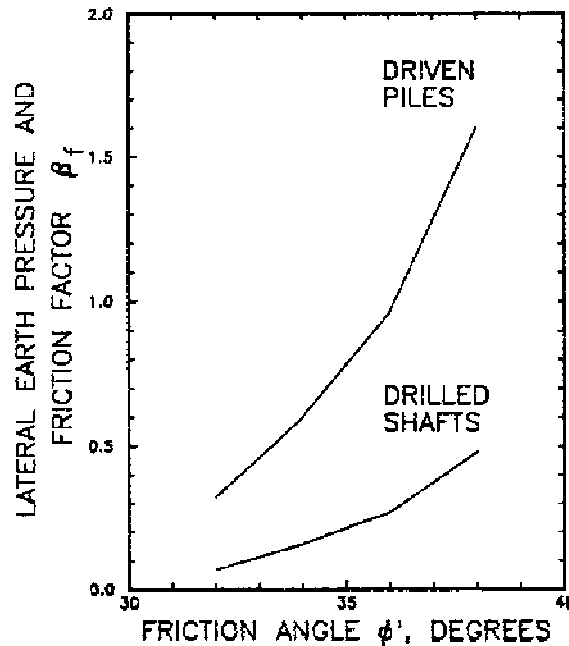


Figure 5-5. Lateral earth pressure and friction angle factor β as a function of friction angle prior to installation (Data from Meyerhof 1976 and Poulos and Davis 1980)

(b) Refer to Figure 5-3 to determine the critical depth L_c below which σ'_i remains constant with increasing depth.

(3) **CPT Field Estimate.** The skin friction f_{si} may be estimated from the measured cone resistance q_c for the piles described in Table 5-2 using the curves given in Figure 5-6 for clays and silt, sands and gravels, and chalk (Bustamante and Gianeselli 1983).

c. **Example Application.** A 1.5-ft diameter straight concrete drilled shaft is to be constructed 30 ft deep through a 2-layer soil of a slightly overconsolidated clay with $PI = 40$ and fine uniform sand, Figure 5-7. Depth of embedment in the sand layer $L_b = 15$ ft. The water table is 15 ft below ground surface at the clay-sand interface. The concrete unit weight $\gamma_{conc} = 150$ lbs/ft³. Design load $Q_d = 75$ kips.

TABLE 5-2

Descriptions of Deep Foundations. Note that the curves matching the numbers are found in Figure 5-6. (Data from Bustamante and Gianeselli 1983)

a. Drilled Shafts

File	Description	Remarks	Cone Resistance q_c , ksf	Soil	Curve
Drilled shaft bored dry	Hole bored dry without slurry; applicable to cohesive soil above water table	Tool without teeth; oversize blades; remolded soil on sides	any	Clay-Silt	1
		Tool with teeth; immediate concrete placement	> 25	Clay-Silt	2
			> 94	Clay-Silt	3
			any	Chalk	1
		Immediate concrete placement	> 94	Chalk	3
		Immediate concrete placement with load test	>250	Chalk	4
Drilled shaft with slurry	Slurry supports sides; concrete placed through tremie from bottom up displacing	Tool without teeth; oversize blades; remolded soil on sides	any	Clay-Silt	1
		Tool with teeth; immediate concrete placement	> 25	Clay-Silt	2
			> 94	Clay-Silt	3
			any	Sand-Gravel	1
		Fine sands and length < 100 ft	>104	Sand-Gravel	2
		Coarse gravelly sand/gravel and length < 100 ft	>156	Sand-Gravel	3
		Gravel	> 83	Sand-Gravel	4
			any	Chalk	1
		Above water table; immediate concrete placement	> 94	Chalk	3
		Above water table; immediate concrete placement with load test	>250	Chalk	4
Drilled shaft with casing	Bored within steel casing; concrete placed as casing retrieved	Dry holes	any	Clay-Silt	1
			> 25	Clay-Silt	2
			any	Sand-Gravel	1
		Fine sands and length < 100 ft	> 104	Sand-Gravel	2
		Coarse sand/gravel and length < 100 ft	>157	Sand-Gravel	3
		Gravel	> 83	Sand-Gravel	4
			any	Chalk	1
		Above water table; immediate concrete placement	> 94	Chalk	3
Drilled shaft hollow auger (auger cast pile)	Hollow stem continuous auger length > shaft length; auger extracted without turning while concrete injected through auger stem		any	Clay-Silt	1
			> 25	Clay-Silt	2
			any	Sand-Gravel	1
		Sand exhibiting some cohesion	>104	Sand-Gravel	2
			any	Chalk	1
Pier	Hand excavated; sides supported with retaining elements or casing		any	Clay-Silt	1
			> 25	Clay-Silt	2
		Above water table; immediate concrete placement	> 94	Chalk	3
	Above water table; immediate concrete placement	>250	Chalk	4	

TABLE 5-2 (Continued)

File	Description	Remarks	Cone Resistance q_c , ksf	Soil	Curve
Micropile I	Drilled with casing; diameter < 10 in.; casing recovered by applying pressure inside top of plugged casing	With load test	any	Clay-Silt	1
			> 25	Clay-Silt	2
			> 25	Clay-Silt	3
			any	Sand-Gravel	1
			>104	Sand-Gravel	2
			>157	Sand-Gravel	3
			any	Chalk	1
> 94	Chalk	3			
Micropile II	Drilled < 10 in. diameter; reinforcing cage placed in hole and concrete placed from bottom-up	With load test	any	Clay-Silt	1
			> 42	Clay-Silt	4
			> 42	Clay-Silt	5
			>104	Sand-Gravel	5
			> 94	Chalk	4
High pressure injected	Diameter > 10 in. with injection system capable of high pressures	Coarse gravelly sand/gravel	any	Clay-Silt	1
			> 42	Clay-Silt	5
			>104	Sand-Gravel	5
			>157	Sand-Gravel	3
			> 94	Chalk	4

b. Driven Piles

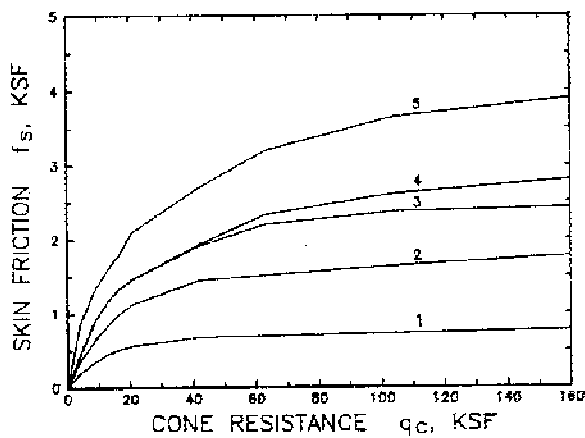
File	Description	Remarks	Cone Resistance q_c , ksf	Soil	Curve	
Screwed-in	Screw type tool placed in front of corru- gated pipe that is pushed or screwed in place; reverse rotation to pull casing while placing concrete		any	Clay-Silt	1	
			$q_c < 53$ ksf	> 25	Clay-Silt	2
			Slow penetration	> 94	Clay-Silt	3
			Slow penetration	any	Sand-Gravel	1
			Fine sands with load test	> 73	Sand-Gravel	2
			Coarse gravelly sand/gravel	>157	Sand-Gravel	3
			Coarse gravelly sand/gravel	any	Chalk	1
			$q_c < 146$ ksf without load test	> 63	Chalk	2
			$q_c < 146$ ksf with load test	> 63	Chalk	3
			Above water table; immediate concrete placement; slow penetration	> 94	Chalk	3
			Above water table with load test	>250	Chalk	4
Concrete coated	6 to 20 in. diameter pipe; H piles; caissons of 2 to 4 sheet pile sections; pile driven with oversize protecting shoe; concrete in- jected through hose near oversize shoe producing coating around pile	With load test	any	Clay-Silt	1	
			any	Sand-Gravel	1	
			>157	Sand-Gravel	4	
			any	Chalk	1	
			> 63	Chalk	3	
			> 94	Chalk	3	
			>250	Chalk	4	

TABLE 5-2 (Continued)

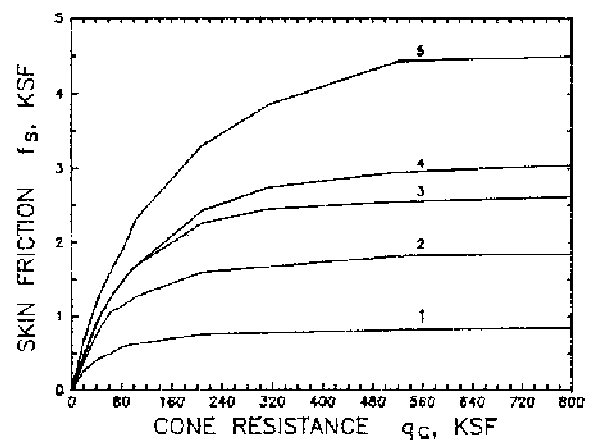
File	Description	Remarks	Cone Resistance q_c , ksf	Soil	Curve
Prefabricated	Reinforced or prestressed concrete installed by driving or vibrodriving		any	Clay-Silt	1
			any	Sand-Gravel	1
		Fine Sands	>157	Sand-Gravel	2
		Coarse gravelly sand/gravel	>157	Sand-Gravel	3
		With load test	>157	Sand-Gravel	4
			any	Chalk	1
		$q_c < 147$ ksf without load test	> 63	Chalk	2
		$q_c < 147$ ksf with load test	> 63	Chalk	3
		With load test	>250	Chalk	4
Steel	H piles; pipe piles; any shape obtained by welding sheet-pile sections		any	Clay-Silt	1
			any	Sand-Gravel	1
		Fine sands with load test	> 73	Sand-Gravel	2
		Coarse gravelly sand/gravel	>157	Sand-Gravel	3
			any	Chalk	1
		$q_c < 147$ ksf without load test	> 63	Chalk	2
$q_c < 147$ ksf with load test	> 63	Chalk	3		
Prestressed tube	Hollow cylinder element of lightly reinforced concrete assembled by prestressing before driving; 4-9 ft long elements; 2-3 ft diameter; 6 in. thick; piles driven open ended		any	Clay-Silt	1
			any	Sand-Gravel	1
		With load test	> 73	Sand-Gravel	2
		Fine sands with load test	>157	Sand-Gravel	2
		Coarse gravelly sand/gravel	>157	Sand-Gravel	3
		With load test	>157	Sand-Gravel	4
			< 63	Chalk	1
		$q_c < 146$ ksf	> 63	Chalk	2
		With load test	> 63	Chalk	3
With load test	>250	Chalk	4		
Concrete plug bottom of Pipe	Driving accomplished through bottom concrete plug; casing pulled while low slump concrete compacted through casing		any	Clay-Silt	1
		$q_c < 42$ ksf	> 25	Clay-Silt	3
			any	Sand-Gravel	1
		Fine sands with load test	> 73	Sand-Gravel	2
			any	Chalk	1
	> 94	Chalk	4		
Molded	Plugged tube driven to final position; tube filled to top with medium slump concrete and tube extracted		any	Clay-Silt	1
		With load test	> 25	Clay-Silt	2
			any	Sand-Gravel	1
		Fine sand with load test	> 73	Sand-Gravel	2
		Coarse gravelly sand/gravel	>157	Sand-Gravel	3
			any	Chalk	1
		$q_c < 157$ ksf	> 63	Chalk	2
		With load test	> 63	Chalk	3
With load test	>250	Chalk	4		
Pushed-in concrete	Cylindrical concrete elements prefabricated or cast-in-place 1.5-8 ft long, 1-2 ft diameter; elements pushed by hydraulic jack		any	Clay-Silt	1
			any	Sand-Gravel	1
		Fine sands	>157	Sand-Gravel	2
		Coarse gravelly sand/gravel	>157	Sand-Gravel	3
		Coarse gravelly sand/gravel with load test	>157	Sand-Gravel	4
			any	Chalk	1
		$q_c < 157$ ksf	> 63	Chalk	2
		With load test	> 63	Chalk	3
With load test	>250	Chalk	4		

TABLE 5-2 (Concluded)

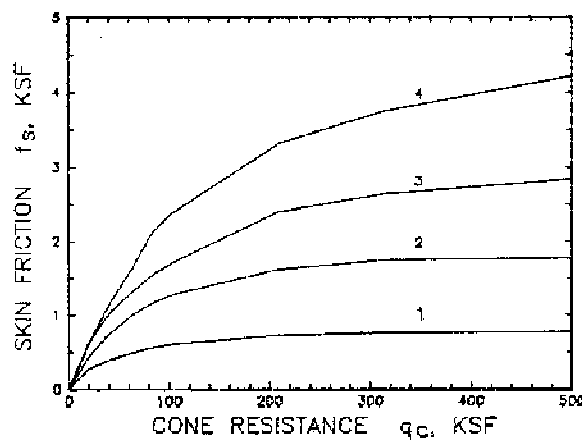
File	Description	Remarks	Cone Resistance q_c , ksf	Soil	Curve
Pushed-in steel	Steel piles pushed in by hydraulic jack		any	Clay-Silt	1
			any	Sand-Gravel	1
		Coarse gravelly sand/gravel	>157	Sand-Gravel	3
			any	Chalk	1
		$q_c < 157$ ksf With load test	> 63	Chalk	2
			>250	Chalk	4



a. CLAY AND SILT



b. SAND AND GRAVEL



c. CHALK

Figure 5-6. Skin friction and cone resistance relationships for deep foundations (Data from Bustamante and Gianselli 1983).
The appropriate curve to use is determined from Table 5-2

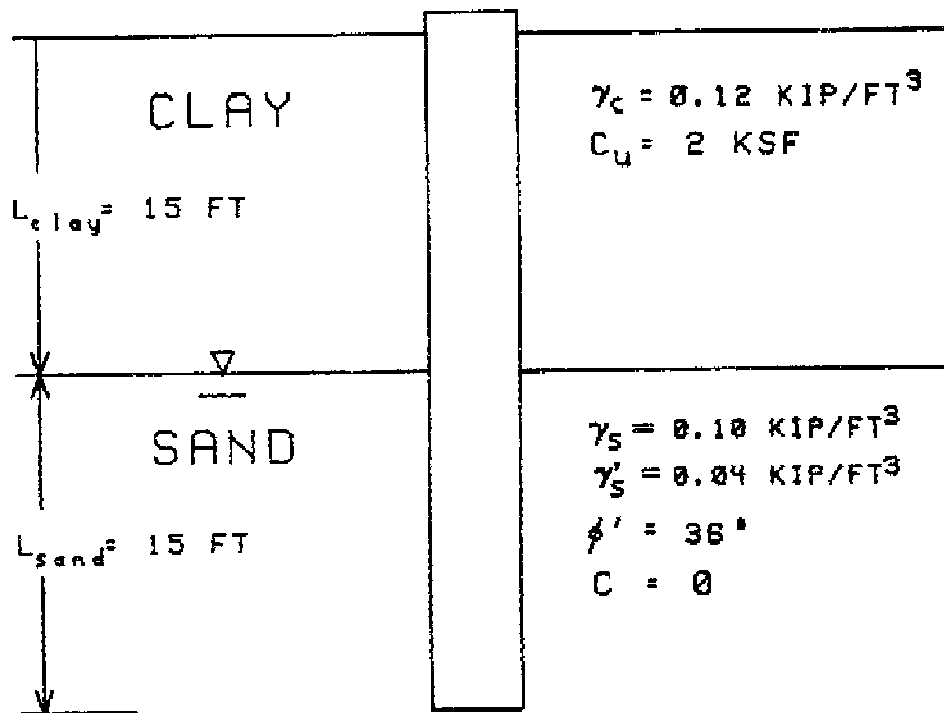


Figure 5-7. Drilled shaft 1.5-ft diameter at 30-ft depth

(1) **Soil Parameters.**

(a) The mean effective vertical stress in a soil layer σ'_s such as in a sand layer below a surface layer, Figure 5-7, may be estimated by

$$\sigma'_s = L_{clay} \gamma'_c + \frac{L_{sand}}{2} \gamma'_s \quad (5-13a)$$

where

- L_{clay} = thickness of a surface clay layer, ft
- γ'_c = effective unit weight of surface clay layer, kips/ft³
- L_{sand} = thickness of an underlying sand clay layer, ft
- γ'_s = effective wet unit weight of underlying sand layer, kips/ft³

The mean effective vertical stress in the sand layer adjacent to the embedded pile from Equation 5-13a is

The effective vertical soil stress at the pile tip is

$$\begin{aligned} \sigma'_s &= L_{clay} \gamma'_c + \frac{L_{sand}}{2} \gamma'_s = 15 \cdot 0.12 + \frac{15}{2} \cdot 0.04 = 1.8 + 0.3 \\ \sigma'_s &= 2.1 \text{ ksf} \quad \sigma'_L = L_{clay} \gamma'_c + L_{sand} \gamma'_s \\ &= 15 \cdot 0.12 + 15 \cdot 0.04 \\ &= 1.8 + 0.6 = 2.4 \text{ ksf} \end{aligned} \quad (5-13b)$$

(b) Laboratory strength tests indicate that the average undrained shear strength of the clay is $C_u = 2$ ksf. Cone penetration tests indicate an average cone tip resistance q_c in the clay is 40 ksf and in the sand 160 ksf.

(c) Relative density of the sand at the shaft tip is estimated from Equation 3-5

$$D_r = -74 + 66 \cdot \log_{10} \frac{q_c}{(\sigma'_{vo})^{0.5}} = -74 + 66 \cdot \log_{10} \frac{160}{(2.4)^{0.5}}$$

$$D_r = -74 + 133 = 59 \text{ percent}$$

The effective friction angle estimated from Table 3-1a is $\phi' = 38$ deg, while Table 3-1b indicates $\phi' = 36$ to 38 deg. Figure 3-1 indicates $\phi' = 38$ deg. The sand appears to be of medium to dense density. Select a conservative $\phi = 36$ deg. Coefficient of earth pressure at rest from the Jaky Equation 5-6c is $K_o = 1 - \sin \phi = 1 - \sin 36 \text{ deg} = 0.42$.

(d) The sand elastic modulus E_s is at least 250 ksf from Table D-3 in EM 1110-1-1904 using guidelines for a medium to dense sand. The shear modulus G_s is estimated using $G_s = E_s / [2(1 + \nu_s)] = 250 / [2(1 + 0.3)] = 96$ or approximately 100 ksf. Poisson's ratio of the sand $\nu_s = 0.3$.

(2) **End Bearing Capacity.** A suitable estimate of end bearing capacity q_{bu} for the pile tip in the sand may be evaluated from the various methods in 5-2a for cohesionless soil as described below. Hanson and Vesic methods account for a limiting effective stress, while the general shear method and Vesic alternate method ignore this stress. The Vesic Alternate method is not used because the sand appears to be of medium density and not loose. Local shear failure is not likely.

(a) Hansen Method. From Table 4-4 (or calculated from Table 4-5), $N_{qp} = 37.75$ and $N_{\gamma p} = 40.05$ for $\phi' = 36$ deg. From Table 4-5,

$$\zeta_{qs} = 1 + \tan \phi = 1 + \tan 36 = 1.727$$

$$\zeta_{qd} = 1 + 2 \tan \phi (1 - \sin \phi)^2 \cdot \tan^{-1}(L_{\text{sand}}/B)$$

$$= 1 + 2 \tan 36 (1 - \sin 36)^2 \cdot \tan^{-1}(15/1.5) \cdot \pi/180$$

$$= 1 + 2 \cdot 0.727 (1 - 0.588)^2 \cdot 1.471 = 1.363$$

$$\zeta_{qp} = \zeta_{qs} \cdot \zeta_{qd} = 1.727 \cdot 1.363 = 2.354$$

$$\zeta_{\gamma s} = 1 - 0.4 = 0.6$$

$$\zeta_{\gamma d} = 1.00$$

$$\zeta_{\gamma p} = \zeta_{\gamma s} \cdot \zeta_{\gamma d} = 0.6 \cdot 1.00 = 0.6$$

From Equation 5-2a

$$q_{bu} = \sigma'_v \cdot N_{qp} \zeta_{qp} + \frac{B_p}{2} \cdot \gamma'_b \cdot N_{\gamma p} \zeta_{\gamma p}$$

$$= 2.4 \cdot 37.75 \cdot 2.354 + \frac{1.5}{2} \cdot 0.04 \cdot 40.05 \cdot 0.6$$

$$= 213.3 + 0.7 = 214 \text{ ksf}$$

(b) Vesic Method. The reduced rigidity index from Equation 5-5c is

$$I_{rr} = \frac{I_r}{1 + \epsilon_v \cdot I_r} = \frac{57.3}{1 + 0.006 \cdot 57.3} = 42.6$$

where

$$\epsilon_v = \frac{1 - 2\nu_s}{2(1 - \nu_s)} \cdot \frac{\sigma'_L}{G_s} = \frac{1 - 2 \cdot 0.3}{2(1 - 0.3)} \cdot \frac{2.4}{100} = 0.006 \quad (5-5e)$$

$$I_r = \frac{G_s}{c + \sigma'_L \tan \phi'} = \frac{100}{2.4 \cdot \tan 36} = 57.3 \quad (5-5d)$$

From Equation 5-5b

$$\begin{aligned} N_{qp} &= \frac{3}{3 - \sin \phi'} \cdot e^{\frac{(90 - \phi') \pi \tan \phi'}{180}} \cdot \tan^2 \left[45 + \frac{\phi'}{2} \right] \cdot I_{rr}^{\frac{4 \sin \phi'}{3(1 + \sin \phi')}} \\ &= \frac{3}{3 - \sin 36} \cdot e^{\frac{(90 - 36) \pi \tan 36}{180}} \cdot \tan^2 \left[45 + \frac{36}{2} \right] \cdot I_{rr}^{\frac{4 \sin 36}{3(1 + \sin 36)}} \\ N_{qp} &= \frac{3}{3 - 0.588} \cdot e^{0.685 \cdot 3.852} \cdot 42.6^{0.494} \\ &= 1.244 \cdot 1.984 \cdot 3.852 \cdot 6.382 = 60.7 \end{aligned}$$

The shape factor from Equation 5-6a is

$$\zeta_{qp} = \frac{1 + 2K_o}{3} = \frac{1 + 2 \cdot 0.42}{3} = 0.61$$

From Equation 5-2c,

$$q_{bu} = \sigma'_L \cdot N_{qp} \cdot \zeta_{qp} = 2.4 \cdot 60.7 \cdot 0.61 = 88.9 \text{ ksf}$$

(c) General Shear Method. From Equation 5-8

$$\begin{aligned} N_{qp} &= \frac{e^{\frac{270 - \phi'}{180} \cdot \pi \cdot \tan \phi'}}{2 \cdot \cos^2 \left[45 + \frac{\phi'}{2} \right]} = \frac{e^{\frac{270 - 36}{180} \cdot \pi \cdot \tan 36}}{2 \cdot \cos^2 \left[45 + \frac{36}{2} \right]} \\ &= \frac{e^{1.3 \pi \cdot 0.727}}{2 \cdot 0.206} = 47.24 \end{aligned}$$

The shape factor $\zeta_{qp} = 1.00$ when using Equation 5-8. From Equation 5-2c,

$$q_{bu} = \sigma'_L \cdot N_{qp} \cdot \zeta_{qp} = 2.4 \cdot 47.24 \cdot 1.00 = 113.4 \text{ ksf}$$

(d) Comparison of Methods. A comparison of methods is shown as follows:

Method	q_{bu} , ksf
Hansen	214
Vesic	89
General Shear	113

The Hansen result of 214 ksf is much higher than the other methods and should be discarded without proof from a load test. The Vesic and General Shear methods give an average value $q_{bu} = 102$ ksf.

(2) **Skin Friction Capacity.** A suitable estimate of skin friction f_s from the soil-shaft interface may be evaluated by methods in Section 5-2b for embedment of the shaft in both clay and sand as illustrated below.

(a) Cohesive Soil. The average skin friction from Equation 5-10 is

$$f_s = \alpha_a \cdot C_u = 0.5 \cdot 2 = 1.0 \text{ ksf}$$

where α_a was estimated from Equation 5-11b, $\alpha_a = 0.9 - 0.01 \cdot 40 = 0.5$ or 0.55 from Table 5-1. Skin friction from the top 5 ft should be neglected.

(b) Cohesionless Soil. Effective stresses are limited by $L_c/B = 10$ or to depth $L_c = 15$ ft. Therefore, $\sigma'_s = 1.8$ ksf, the effective stress at 15 ft. The average skin friction from Equation 5-12a is

$$f_s = \beta_f \cdot \sigma'_s = 0.26 \cdot 1.8 = 0.5 \text{ ksf}$$

where $\beta_f = 0.26$ from Figure 5-5 using $\phi' = 36$ deg.

(c) CPT Field Estimate. The shaft was bored using bentonite-water slurry. Use curve 2 of clay and silt, Figure 5-6a, and curve 3 of sand and gravel, Figure 5-6b. From these figures, f_s of the clay is 1.5 ksf and f_s of the sand is 2.0 ksf.

(d) Comparison of Methods. Skin friction varies from 1.0 to 1.5 ksf for the clay and 0.5 to 2 ksf for the sand. Skin friction is taken as 1 ksf in the clay and 1 ksf in the sand, which is considered conservative.

(3) **Total Capacity.** The total bearing capacity from Equation 5-1a is

$$Q_u = Q_{bu} + Q_{su} - W_p$$

where

$$\begin{aligned} W_p &= \frac{\pi B^2}{4} \cdot L_{clay} \gamma_{conc} + \frac{\pi B^2}{4} \cdot L_{sand} \gamma'_{conc} \\ &= \frac{\pi 1.5^2}{4} \cdot \left[15 \cdot \frac{150}{1000} + 15 \cdot \frac{86}{1000} \right] \\ &= 4.0 + 2.3 = 6.3 \text{ kips} \end{aligned}$$

γ_{conc} is the unit weight of concrete, 150 lbs/ft³.

(a) Q_{bu} from Equation 5-1b is

$$Q_{bu} = q_{bu} \cdot A_b = 102 \cdot 1.77 = 180 \text{ kips}$$

where $A_b =$ area of the base, $\pi B^2/4 = \pi \cdot 1.5^2/4 = 1.77$ ft².

EM 1110-1-1905
30 Oct 92

(b) Q_{su} from Equation 5-1b and 5-9

$$Q_{su} = \sum_{i=1}^n Q_{sui} = C_s \cdot \Delta L \sum_{i=1}^2 f_{si}$$

where $C_s = \pi B$ and $\Delta L = 15$ ft for clay and 15 ft for sand. Therefore,

$$\begin{aligned} Q_{su} &= \pi \cdot B \cdot [\Delta L \cdot f_s^{\text{sand}} + \Delta L \cdot f_s^{\text{clay}}] \\ &= \pi \cdot 1.5 \cdot [15 \cdot 1 + 10 \cdot 1] = 118 \text{ kips} \end{aligned}$$

where skin friction is ignored in the top 5 ft of clay.

(c) **Total Capacity.** Inserting the end bearing and skin resistance bearing capacity values into Equation 5-1a is

$$Q_u = 180 + 118 - 6 = 292 \text{ kips}$$

(4) **Allowable Bearing Capacity.** The allowable bearing capacity from Equation 1-2b is

$$Q_a = \frac{Q_u}{FS} = \frac{292}{3} = 97 \text{ kips}$$

using $FS = 3$ from Table 1-2. $Q_d = 75 < Q_a = 97$ kips. A settlement analysis should also be performed to check that settlement is tolerable. A load test is recommended to confirm or correct the ultimate bearing capacity. Load tests can increase Q_a because $FS = 2$ and permit larger Q_d depending on results of settlement analysis.

d. Load Tests for Vertical Capacity. ASTM D 1143 testing procedures for piles under static compression loads are recommended and should be performed for individual or groups of vertical and batter shafts (or piles) to determine their response to axially applied compression loads. Load tests lead to the most efficient use of shafts or piles. The purpose of testing is to verify that the actual pile response to compression loads corresponds to that used for design and that the calculated ultimate load is less than the actual ultimate load. A load cell placed at the bottom of the shaft can be used to determine the end bearing resistance and to calculate skin friction as the difference between the total capacity and end bearing resistance.

(1) **Quick Load Test.** The "Quick" load test option is normally satisfactory, except that this test should be taken to plunging failure or three times the design load or 1000 tons, whichever comes first.

(2) **Cost Savings.** Load tests can potentially lead to significant savings in foundation costs, particularly on large construction projects when a substantial part of the bearing capacity is contributed by skin friction. Load tests also assist the selection of the best type of shaft or pile and installation depth.

(3) **Lower Factor of Safety.** Load tests allow use of a lower safety factor of 2 and can offer a higher allowable capacity.

(4) **Scheduling of Load Tests.** Load tests are recommended during the design phase, when economically feasible, to assist in selection of optimum equipment for construction and driving the piles in addition to verifying the bearing capacity. This information can reduce contingency costs in bids and reduce the potential for later claims.

(a) Load tests are recommended for most projects during early construction to verify that the allowable loads used for design are appropriate and that installation procedures are satisfactory.

(b) Load tests during the design phase are economically feasible for large projects such as for multistory structures, power plants, locks and dams.

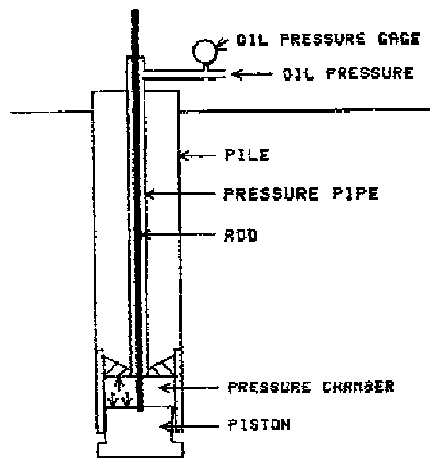
(c) When load tests are performed during the design phase, care must be taken to ensure that the same procedures and equipment (or driving equipment including hammer, helmet, cushion, etc. in the case of driven piles) are used in actual construction.

(5) **Alternative Testing Device.** A load testing device referred to as the Osterberg method (Osterberg 1984) can be used to test both driven piles and drilled shafts. A piston is placed at the bottom of the bored shaft before the concrete is placed or the piston can be mounted at the bottom of a pile, Figure 5-8a. Pressure is applied to hydraulic fluid which fills a pipe leading to the piston. Fluid passes through the annular space between the rod and pressure pipe into the pressure chamber. Hydraulic pressure expands the pressure chamber forcing the piston down. This pressure is measured by the oil (fluid) pressure gage, which can be calibrated to determine the force applied to the bottom of the pile and top of the piston. End bearing capacity can be determined if the skin friction capacity exceeds the end bearing capacity; this condition is frequently not satisfied.

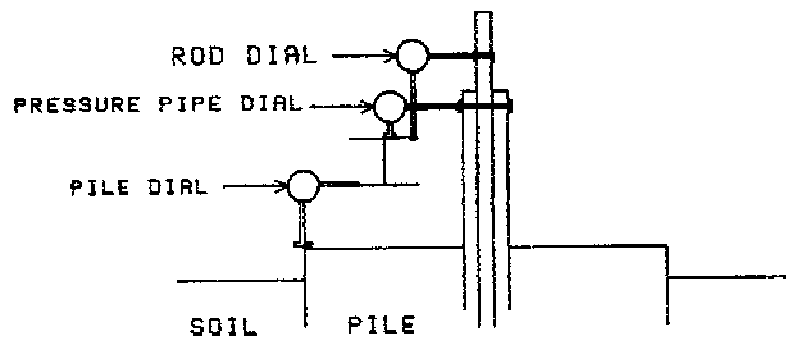
(a) A dial attached to the rod with the stem on the reference beam, Figure 5-8b, measures the downward movement of the piston. A dial attached to the pressure pipe measures the upward movement of the pile base. A third dial attached to the reference beam with stem on the pile top measures the movement of the pile top. The difference in readings between the top and bottom of the pile is the elastic compression due to side friction. The total side friction force can be estimated using Young's modulus of the pile.

(b) If the pile is tested to failure, the measured force at failure (piston downward movement is continuous with time or excessive according to guidance in Table 5-3) is the ultimate end bearing capacity. The measured failure force in the downward plunging piston therefore provides a FS > 2 against failure considering that the skin friction capacity is equal to or greater than the end bearing capacity.

(c) This test can be more economical and completed more quickly than a conventional load test; friction and end bearing resistance can be determined separately; optimum length of driven piles can be determined by testing the same pile at successfully deeper depths. Other advantages include ability to work over water, to work in crowded and inaccessible locations, to test battered piles, and to check pullout capacity as well as downward load capacity.



a. LOAD CELL ARRANGEMENT



b. DIAL GAGE ARRANGEMENT

Figure 5-8. Example load test arrangement for Osterberg method

(6) **Analysis of Load Tests.** Table 5-3 illustrates four methods of estimating ultimate bearing capacity of a pile from data that may be obtained from a load-displacement test such as described in ASTM D 1143. At least three of these methods, depending on local experience or preference, should be used to determine a suitable range of probable bearing capacity. The methods given in Table 5-3 give a range of ultimate pile capacities varying from 320 to 467 kips for the same pile load test data.

5-3. **Capacity to Resist Uplift and Downdrag.** Deep foundations may be subject to other vertical loads such as uplift and downdrag forces. Uplift forces are caused by pullout loads from structures or heave of expansive soils surrounding the shaft tending to drag the shaft up. Downdrag forces are caused by settlement of soil surrounding the shaft that exceeds the downward displacement of the shaft and increases the downward load on the shaft. These forces influence the skin friction that is developed between the soil and the shaft perimeter and influences bearing capacity.

TABLE 5-3

Methods of Estimating Ultimate Bearing Capacity From Load Tests

Method	Procedure	Diagram
Tangent (Butler and Hoy 1977)	<ol style="list-style-type: none"> 1. Draw a tangent line to the curve at the graph's origin 2. Draw another tangent line to the curve with slope equivalent to slope of 1 inch for 40 kips of load 3. Ultimate bearing capacity is the load at the intersection of the tangent lines 	
Limit Value (Davisson 1972)	<ol style="list-style-type: none"> 1. Draw a line with slope $\frac{\pi B^2}{4L} E_p$ where B = diameter of pile, inches; E_p = Young's pile modulus, kips/inch²; L = pile length, inches 	
B/120	<ol style="list-style-type: none"> 2. Draw a line parallel with the first line starting at a displacement of 0.15 + inch at zero load 3. Ultimate bearing capacity is the load at the intersection of the load-displacement curve with the line of step 2 	

TABLE 5-3 (Concluded)

Method	Procedure	Diagram
80 Percent (Hansen 1963)	<ol style="list-style-type: none"> Plot load test results as $\frac{\sqrt{p}}{Q}$ vs. p Draw straight line through data points Determine the slope a and intercept b of this line Ultimate bearing capacity is $Q_u = \frac{1}{2\sqrt{ab}}$ Ultimate deflection is $p_u = b/a$ 	
90 Percent (Hansen 1963)	<ol style="list-style-type: none"> Calculate $0.9Q$ for each load Q Find $p_{0.90}$, displacement for load of $0.9Q$, for each Q from Q vs. p plot Determine $2p_{0.90}$ for each Q and plot vs. Q on chart with the load test data of Q vs. p Ultimate bearing capacity is the load at the intersection of the two plots of data 	

a. **Method of Analysis.** Analysis of bearing capacity with respect to these vertical forces requires an estimate of the relative movement between the soil and the shaft perimeter and the location of neutral point n , the position along the shaft length where there is no relative movement between the soil and the shaft. In addition, tension or compression stresses in the shaft or pile caused by uplift or downdrag must be calculated to properly design the shaft. These calculations are time-dependent and complicated by soil movement. Background theory for analysis of pullout, uplift and downdrag forces of single circular drilled shafts, and a method for computer analysis of these forces is provided below. Other methods of

evaluating vertical capacity for uplift and downdrag loads are given in Reese and O'Neill (1988).

b. **Pullout.** Deep foundations are frequently used as anchors to resist pullout forces. Pullout forces are caused by overturning moments such as from wind loads on tall structures, utility poles, or communication towers.

(1) **Force Distribution.** Deep foundations may resist pullout forces by shaft skin resistance and resistance mobilized at the tip contributed by enlarged bases illustrated in Figure 5-9. The shaft resistance is defined in terms of negative skin friction f_n to indicate that the shaft is moving up relative to the soil. This is in contrast to compressive loads that are resisted by positive skin friction where the shaft moves down relative to the soil, Figure 5-4. The shaft develops a tensile stress from pullout forces. Bearing capacity resisting pullout may be estimated by

$$P_u = Q_{bu} + P_{nu} + W_p \quad (5-14a)$$

$$P_u = q_{bu}A_{bp} + \sum_{i=1}^n P_{nu_i} + W_p \quad (5-14b)$$

where

P_u = ultimate pullout resistance, kips
 A_{bp} = area of base resisting pullout force, ft²
 P_{nu_i} = pullout skin resistance for pile element i , kips

(2) **End Bearing Resistance.** Enlarged bases of drilled shafts resist pullout and uplift forces. q_{bu} may be estimated using Equation 5-2c. Base area A_b resisting pullout to be used in Equation 5-1b for underreamed drilled shafts is

$$A_{bp} = \frac{\pi}{4} \cdot (B_b^2 - B_s^2) \quad (5-15)$$

where

B_b = diameter of base, ft
 B_s = diameter of shaft, ft

(a) **Cohesive Soil.** The undrained shear strength C_u to be used in Equation 5-3 is the average strength above the base to a distance of $2B_b$. N_{cp} varies from 0 at the ground surface to a maximum of 9 at a depth of $2.5B_b$ below the ground (Vesic 1971).

(b) **Cohesionless Soil.** N_{qp} of Equation 5-2 can be obtained from Equation 5-7 of the Vesic alternate method where ζ_{qp} is given by Equations 5-6.

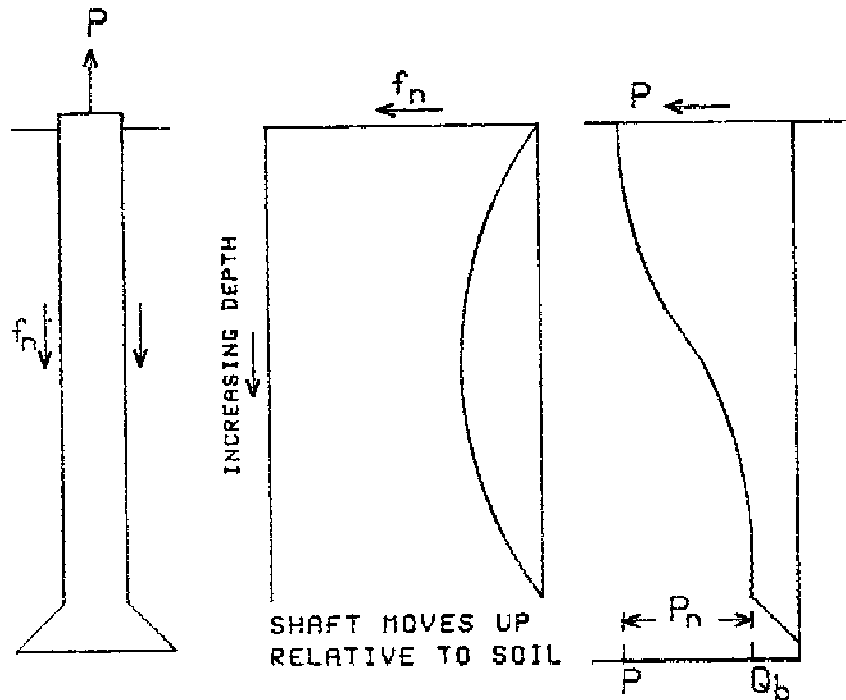


Figure 5-9. Underreamed drilled shaft resisting pullout

(3) **Skin Resistance.** The diameter of the shaft may be slightly reduced from pullout forces by a Poisson effect that reduces lateral earth pressure on the shaft perimeter. Skin resistance will therefore be less than that developed for shafts subject to compression loads because horizontal stress is slightly reduced. The mobilized negative skin friction f_{ni} may be estimated as 2/3 of that evaluated for compression loads f_{si}

$$\sum_{i=1}^n P_{nui} = C_s \cdot \Delta L \sum_{i=1}^n f_{ni} \quad (5-16a)$$

$$f_{ni} = \frac{2}{3} \cdot f_{si} \quad (5-16b)$$

where

C_s = shaft circumference, ft

ΔL = length of pile element i , ft

f_{si} = positive skin friction of element i from compressive loading using Equations 5-10 to 5-12

The sum of the elements equals the shaft length.

c. **Uplift.** Deep foundations constructed in expansive soil are subject to uplift forces caused by swelling of expansive soil adjacent to the shaft. These uplift forces cause a friction on the upper length of the shaft perimeter tending to move the shaft up. The shaft perimeter subject to uplift thrust is in the soil

subject to heave. This soil is often within the top 7 to 20 ft of the soil profile referred to as the depth of the active zone for heave Z_a . The shaft located within Z_a is sometimes constructed to isolate the shaft perimeter from the expansive soil to reduce this uplift thrust. The shaft base and underream resisting uplift should be located below the depth of heaving soil.

(1) **Force Distribution.** The shaft moves down relative to the soil above neutral point n , Figure 5-10, and moves up relative to the soil below point n . The negative skin friction f_n below point n and enlarged bases of drilled shafts resist the uplift thrust of expansive soil. The positive skin friction f_s above point n contributes to uplift thrust from heaving soil and puts the shaft in tension. End bearing and skin friction capacity resisting uplift thrust may be estimated by Equations 5-14.

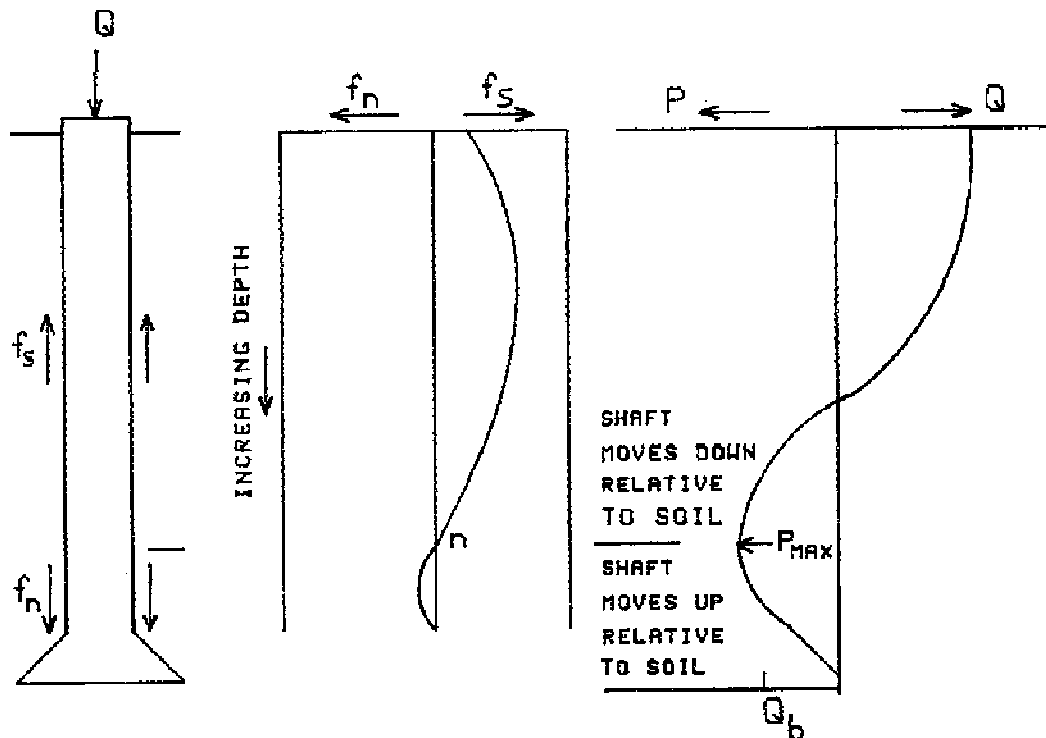


Figure 5-10. Deep foundation resisting uplift thrust

(2) **End Bearing.** End bearing resistance may be estimated similar to that for pullout forces. N_{cp} should be assumed to vary from 0 at the depth of the active zone of heaving soil to 9 at a depth $2.5B_b$ below the depth of the active zone of heave. The depth of heaving soil may be at the bottom of the expansive soil layer or it may be estimated by guidelines provided in TM 5-818-7, EM 1110-1-1904, or McKeen and Johnson (1990).

(3) **Skin Friction.** Skin friction from the top of the shaft to the neutral point n contributes to uplift thrust, while skin friction from point n to the base contributes to skin friction that resists the uplift thrust.

(a) The magnitude of skin friction f_s above point n that contributes to uplift thrust will be as much or greater than that estimated for compression loads. The adhesion factor α_a of Equation 5-10 can vary from 0.6 to 1.0 and can contribute to shaft heave when expansive soil is at or near the ground surface. α_a should not be underestimated when calculating the potential for uplift thrust; otherwise, tension, steel reinforcement, and shaft heave can be underestimated.

(b) Skin friction resistance f_n that resists uplift thrust should be estimated similar to that for pullout loads because uplift thrust places the shaft in tension tending to pull the shaft out of the ground and may slightly reduce lateral pressure below neutral point n .

d. **Downdrag.** Deep foundations constructed through compressible soils and fills can be subject to an additional downdrag force. This downdrag force is caused by the soil surrounding the drilled shaft or pile settling downward more than the deep foundation. The deep foundation is dragged downward as the soil moves down. The downward load applied to the shaft is significantly increased and can even cause a structural failure of the shaft as well as excessive settlement of the foundation. Settlement of the soil after installation of the deep foundation can be caused by the weight of overlying fill, settlement of poorly compacted fill and lowering of the groundwater level. The effects of downdrag can be reduced by isolating the shaft from the soil, use of a bituminous coating or allowing the consolidating soil to settle before construction. Downdrag loads can be considered by adding these to column loads.

(1) **Force Distribution.** The shaft moves up relative to the soil above point n , Figure 5-11, and moves down relative to the soil below point n . The positive skin friction f_s below point n and end bearing capacity resists the downward loads applied to the shaft by the settling soil and the structural loads. Negative skin friction f_n above the neutral point contributes to the downdrag load and increases the compressive stress in the shaft.

(2) **End Bearing.** End bearing capacity may be estimated similar to methods for compressive loads given by Equations 5-2.

(3) **Skin Friction.** Skin friction may be estimated by Equation 5-9 where the positive skin friction is given by Equations 5-10 to 5-12.

e. **Computer Analysis.** Program AXILTR (AXIal Load-TRansfer), Appendix C, is a computer program that computes the vertical shaft and soil displacements for axial down-directed structural, axial pullout, uplift, and down-drag forces using equations in Table 5-4. Load-transfer functions are used to relate base pressures and skin friction with displacements. Refer to Appendix C for example applications using AXILTR for pullout, uplift and downdrag loads.

(1) **Load-Transfer Principle.** Vertical loads are transferred from the top of the shaft to the supporting soil adjacent to the shaft using skin friction-load transfer functions and to soil beneath the base using consolidation theory or base load-transfer functions. The total bearing capacity of the shaft Q_u is the sum of the total skin Q_{su} and base Q_{bu} resistances given by Equations 5-1.

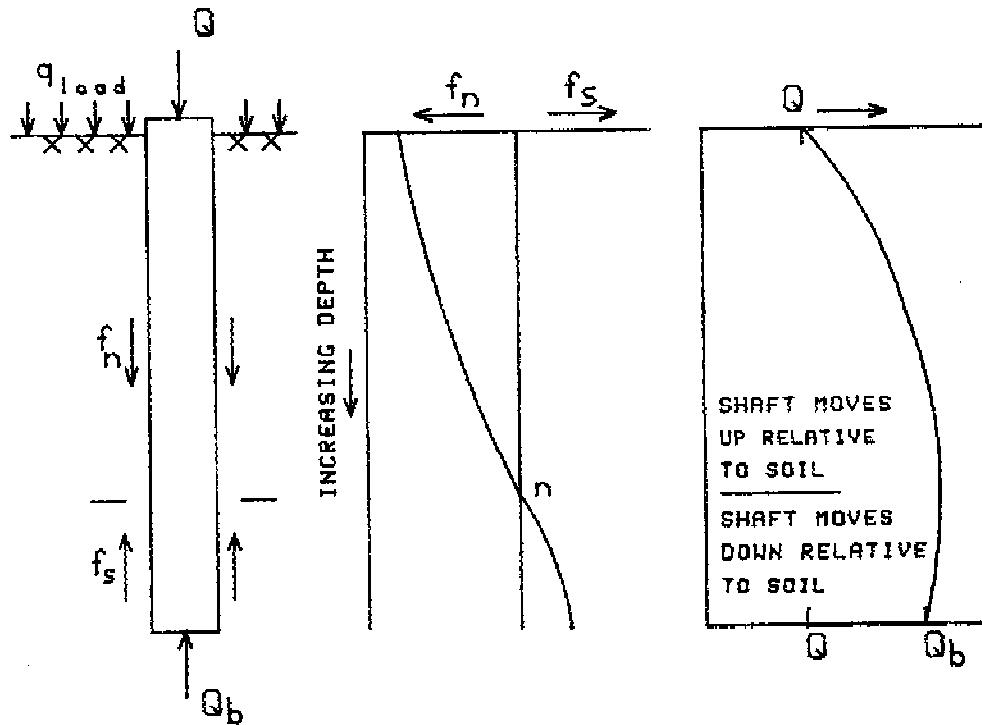


Figure 5-11. Deep foundation resisting downdrag. q_{load} is an area pressure from loads such as adjacent structures

(a) The load-displacement calculations for rapidly applied downward vertical loads have been validated by comparison with field test results (Gurtowski and Wu 1984). The strain distribution from uplift forces for drilled shafts in shrink/swell soil have been validated from results of load tests (Johnson 1984).

(b) The program should be used to provide a minimum and maximum range for the load-displacement behavior of the shaft for given soil conditions. A listing of AXILTR is provided to allow users to update and calibrate this program from results of field experience.

(2) **Base Resistance Load Transfer.** The maximum base resistance q_{bu} in Equation 5-1b is computed by AXILTR from Equation 5-2a

$$q_{bu} = cN_{cp} + \sigma'_L N_{qp} \quad (5-17)$$

where

- c = cohesion, psf
- N_{cp} = cohesion bearing capacity factor, dimensionless
- N_{qp} = friction bearing capacity factor, dimensionless
- σ'_L = effective vertical overburden pressure at the pile base, psf

TABLE 5-4

Program AXILTR Shaft Resistance To Pullout, Uplift and Downdrag Loads

Soil Volume Change	Type of Applied Load	Applied Load, Pounds	Resistance to Applied Load, Pounds	Equations
None	Pullout	$Q_{DL} - P$	Straight: $Q_{sur} + W_p$	$Q_{sur} = \pi B_s \int_0^L f_s dL$
			Underream: Smaller of	$Q_{sub} = \pi B_b \int_0^L \tau_s dL$
			$Q_{sub} + W_p$ $Q_{sur} + Q_{bur} + W_p$	$Q_{sur} = \frac{\pi}{4} c_{bu} B_s^2 (B^2)$ $W_p = L \gamma_p \cdot B^2$
Swelling soil	Uplift thrust	Q_{us}	Straight: $Q_{sur} + W_p$	$Q_{us} = \pi B_s \int_0^{L_n} f_s dL$
			Underream:	$Q_{sur} = \frac{\pi}{4} d B_s \int_{L_n}^L f -$ $Q_{sur} + Q_{bur} + W_p$
Settling soil	Downdrag	$Q_d + Q_{sud}$	$Q_{sur} + Q_{bu}$	$Q_{sud} = \pi B_s \int_0^{L_n} f_n dL$
				$Q_{sur} = \frac{\pi}{4} d B_s \int_{L_n}^L f -$
Nomenclature:				
B_b	Base diameter, ft	Q_{DL}	Dead load of structure, pounds	
B_s	Shaft diameter, ft	P	Pullout load, pounds	
f_s	Maximum mobilized shear strength, psf	Q_{sub}	Ultimate soil shear resistance of cylinder diameter B_b and length equal to depth of underream, pounds	
f_n	Negative skin friction, psf	Q_{sud}	Downdrag, pounds	
L	Shaft length, ft	Q_{sur}	Ultimate skin resistance, pounds	
L_n	Length to neutral point n, ft	Q_{us}	Uplift thrust, pounds	
q_{bu}	Ultimate base resistance, psf	Q_d	Design load, Dead + Live loads, pounds	
Q_{bu}	Ultimate base capacity, pound	W_p	Shaft weight, pounds	
Q_{bur}	Ultimate base resistance of upper portion of underream, pounds	γ_p	Unit shaft weight, pounds/ft ³	
τ_s	Soil shear strength, psf			

Correction factors ζ are assumed unity and the $N_{\gamma p}$ term is assumed negligible. Program AXILTR does not limit σ'_L .

(a) N_{qp} for effective stress analysis is given by Equation 5-7 for local shear (Vesic Alternate method) or Equation 5-8 for general shear.

(b) N_{cp} for effective stress analysis is given by

$$N_{cp} = (N_{qp} - 1) \cot \phi' \quad (5-5a)$$

N_{cp} for total stress analysis is assumed 9 for general shear and 7 for local shear; N_{qp} and total stress friction angle ϕ are zero for total stress analysis.

(c) End bearing resistance may be mobilized and base displacements computed using the Reese and Wright (1977) or Vijayvergiya (1977) base load-transfer functions, Figure 5-12a, or consolidation theory. Ultimate base displacement for the Reese and Wright model is computed by

$$\rho_{bu} = 2B_b \epsilon_{50}^{.12} \quad (5-18)$$

where

ρ_{bu} = ultimate base displacement, in.

B_b = diameter of base, ft

ϵ_{50} = strain at 1/2 of maximum deviator stress of clay from undrained triaxial test, fraction

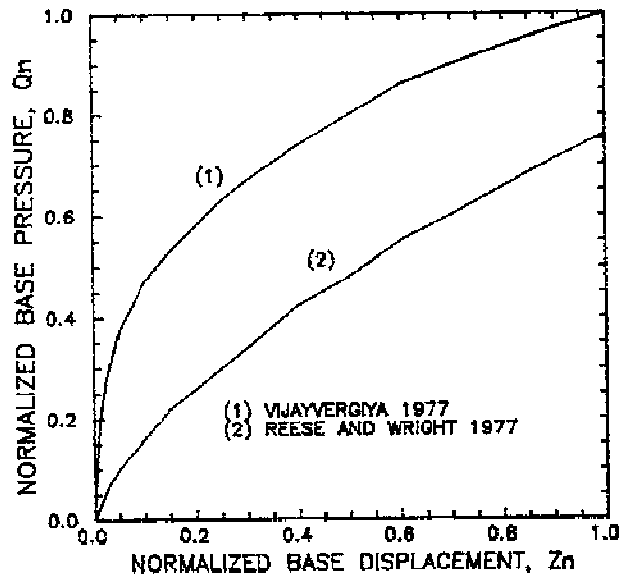
The ultimate base displacement for the Vijayvergiya model is taken as 4 percent of the base diameter.

(d) Base displacement may be calculated from consolidation theory for overconsolidated soils as described in Chapter 3, Section III of EM 1110-1-1904. This calculation assumes no wetting beneath the base of the shaft from exterior water sources, except for the effect of changes in water level elevations. The calculated settlement is based on effective stresses relative to the initial effective pressure on the soil beneath the base of the shaft prior to placement of any structural loads. The effective stresses include any pressure applied to the surface of the soil adjacent to the shaft. AXILTR may calculate large settlements for small applied loads on the shaft if the maximum past pressure is less than the initial effective pressure simulating an underconsolidated soil. Effective stresses in the soil below the shaft base caused by loads in the shaft are attenuated using Boussinesq stress distribution theory (Boussinesq 1885).

(3) **Underream Resistance.** The additional resistance provided by a bell or underream for pullout or uplift forces is 7/9 of the end bearing resistance. If applied downward loads at the base of the shaft exceed the calculated end bearing capacity, AXILTR prints "THE BEARING CAPACITY IS EXCEEDED". If pullout loads exceed the pullout resistance, the program prints "SHAFT PULLS OUT". If the shaft heave exceeds the soil heave, the program prints "SHAFT UNSTABLE".

(4) **Skin Resistance Load Transfer.** The shaft skin friction load-transfer functions applied by program AXILTR are the Seed and Reese (1957) and Kraft, Ray, and Kagawa (1981) models illustrated in Figure 5-12b. The Kraft, Ray, and Kagawa model requires an estimate of a curve fitting constant R from

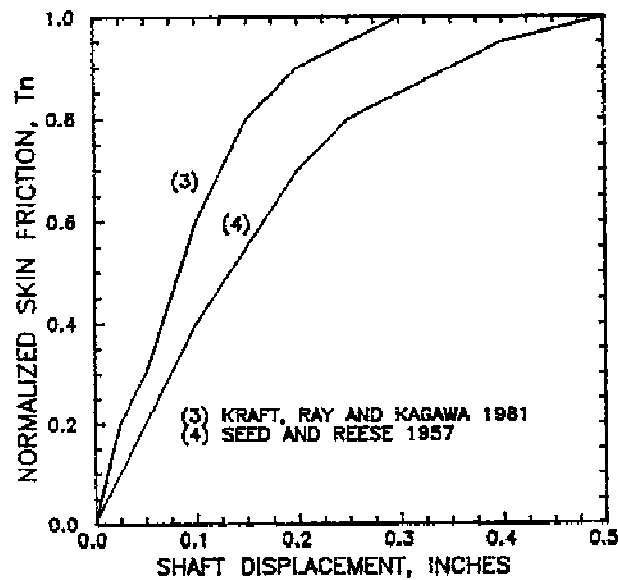
$$G_s = G_i \left[1 - \frac{\tau R}{\tau_{max}} \right] \quad (5-19a)$$



$$Q_n = \frac{\text{BASE PRESSURE } q_b}{\text{ULTIMATE BASE PRESSURE } q_{bu}}$$

$$Z_n = \frac{\text{BASE DISPLACEMENT } \rho_b}{\text{ULTIMATE BASE DISPLACEMENT } \rho_{bu}}$$

a. BASE TRANSFER (NORMALIZED Q-Z) FUNCTIONS



$$T_n = \frac{\text{MOBILIZED SKIN FRICTION } f_s}{\text{MAXIMUM MOBILIZED SKIN FRICTION } f_s^*}$$

b. SHAFT TRANSFER (NORMALIZED T-Z) FUNCTIONS

Figure 5-12. Load-transfer curves applied in AXILTR

where

- G_s = soil shear modulus at an applied shear stress τ , pounds/square foot (psf)
- G_i = initial shear modulus, psf
- τ = shear stress, psf
- τ_{max} = shear stress at failure, psf
- R = curve fitting constant, usually near 1.0

The curve fitting constant R is the slope of the relationship of $1 - G_s/G_i$ versus τ/τ_{max} and may be nearly 1.0. The soil shear modulus G_s is found from the elastic soil modulus E_s by

$$G_s = \frac{E_s}{2(1 + \nu_s)} \quad (5-19b)$$

where ν_s is the soil Poisson's ratio. A good value for ν_s is 0.3 to 0.4.

(a) Load-transfer functions may also be input into AXILTR for each soil layer up to a maximum of 11 different functions. Each load-transfer function consists of 11 data values consisting of the ratio of the mobilized skin friction/maximum mobilized skin friction f_s/f_s^- correlated with displacement as illustrated in Figure 5-12b. The maximum mobilized skin friction f_s^- is assumed the same as the maximum soil shear strength. The corresponding 11 values of the shaft displacement (or shaft movement) in inches are input only once and applicable to all of the load-transfer functions. Therefore, the values of f_s/f_s^- of each load transfer function must be correlated with the given shaft displacement data values.

(b) The full mobilized skin friction f_s^- is computed for effective stresses from

$$f_s^- = c' + \beta_f \sigma'_v \quad (5-20)$$

where

- c' = effective cohesion, psf
- β_f = lateral earth pressure and friction angle factor
- σ'_v = effective vertical stress, psf

The factor β_f is calculated in AXILTR by

$$\beta_f = K_o \tan \phi' \quad (5-21)$$

where

- K_o = lateral coefficient of earth pressure at rest
- ϕ' = effective peak friction angle from triaxial tests, deg

The effective cohesion is usually ignored.

(c) The maximum mobilized skin friction f_s^- for each element is computed for total stresses from Equation 5-10 using α_a from Table 5-1 or Equations 5-11.

(5) **Influence of Soil Movement.** Soil movement, heave or settlement, alters the performance of the shaft. The magnitude of the soil heave or settlement is controlled by the swell or recompression indices, compression indices, maximum past pressure and swell pressure of each soil layer, depth to the water table, and depth of the soil considered active for swell or settlement. The swell index is the slope of the rebound pressure - void ratio curve on a semi-log plot of consolidation test results as described in ASTM D 4546. The recompression index is the slope of the pressure-void ratio curve on a semi-log plot for pressures less than the maximum past pressure. The swell index is assumed identical with the recompression index. The compression index is the slope of the linear portion of the pressure-void ratio curve on a semi-log plot for pressures exceeding the maximum past pressure. The maximum past pressure (preconsolidation stress) is the greatest effective pressure to which a soil has been subjected. Swell pressure is defined as a pressure which prevents a soil from swelling at a given initial void ratio as described by method C in ASTM D 4546.

(a) The magnitude of soil movement is determined by the difference between the initial and final effective stresses in the soil layers and the soil parameters. The final effective stress in the soil is assumed equivalent with the magnitude of the total vertical overburden pressure, an assumption consistent with zero final pore water pressure. Program AXILTR does not calculate soil displacements for shaft load transferred to the soil.

(b) Swell or settlement occurs depending on the difference between the input initial void ratio and the final void ratio determined from the swell and compression indices, the swell pressure, and the final effective stress for each soil element. The method used to calculate soil swell or settlement of soil adjacent to the shaft is described as Method C of ASTM D 4546.

(c) The depth of the active zone Z_a is required and it is defined as the soil depth above which significant changes in water content and soil movement can occur because of climate and environmental changes after construction of the foundation. Refer to EM 1110-1-1904 for further information.

5-4. **Lateral Load Capacity of Single Shafts.** Deep foundations may be subject to lateral loads as well as axial loads. Lateral loads often come from wind forces on the structure or inertia forces from traffic. Lateral load resistance of deep foundations is determined by the lateral resistance of adjacent soil and bending moment resistance of the foundation shaft. The ultimate lateral resistance T_u often develops at lateral displacements much greater than can be allowed by the structure. An allowable lateral load T_a should be determined to be sure that the foundation will be safe with respect to failure.

a. **Ultimate Lateral Load.** Brom's equations given in Table 5-5 can give good results for many situations and these are recommended for an initial estimate of ultimate lateral load T_u . Ultimate lateral loads can be readily determined for complicated soil conditions using a computer program such as COM624G based on beam-column theory and given p-y curves (Reese, Cooley, and Radhakrishnan 1984). A p-y curve is the relationship between the soil resistance per shaft length (kips/inch) and the deflection (inches) for a given lateral load T .

TABLE 5-5

Brom's Equations for Ultimate Lateral Load (Broms 1964a, Broms 1964b, Broms 1965)

a. Free Head Pile in Cohesive Soil

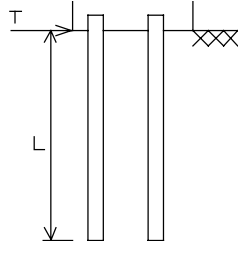
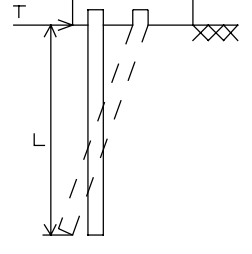
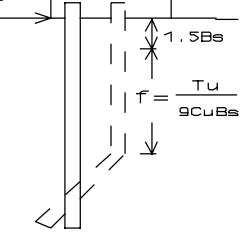
File	Equations	Diagram
Short $L \leq L_c$	$T_u = 18C_uB_s \left[(e^2 + 1.5B_s e + eL + 0.5L^2 + 1.125B_s^2)^{1/2} - (e + 0.75B_s + 0.5L) \right] \quad (5-22a)$	
	$L_c = 1.5B_s + \frac{9}{C_u B_s} + \left[\frac{M_y}{2.25C_u B_s} \right]^{1/2} \quad (5-22b)$	
Long $L \geq L_c$	$T_u = 9C_u B_s \left(\left[(e + 1.5B_s)^2 + \frac{2M_y}{9C_u B_s} \right]^{1/2} - e - 1.5B_s \right) \quad (5-22c)$ <p style="margin-left: 40px;"> <i>Circular:</i> $M_y = 1.3f_y Z$ <i>H-section:</i> $= 1.1f_y Z_{\max}$ <i>H-section:</i> $= 1.5f_y Z_{\min}$ </p>	

b. Free Head Pile in Cohesionless Soil

File	Equations	Diagram
Short $L \leq L_c$	$T_{us} = \frac{\gamma B_s K_p L^3 - 2M_a}{2(e + L)} \quad (5-24a)$	
	$L_c^3 - \frac{2T_{ul}}{\gamma B_s K_p} \cdot L_c - \frac{2(M_a + T_{ul}e)}{\gamma B_s K_p} = 0 \quad (5-24b)$	
Long $L \geq L_c$	$T_{ul} = \frac{M_y - M_a}{e + \frac{2}{3} \cdot f} \quad (5-24c)$	

TABLE 5-5 (Continued)

c. Fixed Head Pile in Cohesive Soil

Pile	Equations	Diagram
Short $L \leq L_{cs}$	$T_u = 9C_u B_s (L - 1.5B_s) \quad (5-23a)$	
	$L_{cs} = 2 \left[\frac{M_y}{18C_u B_s} + \frac{9}{16} \cdot B_s^2 \right] \quad (5-23b)$	
Inter- mediate $L_{cs} \leq L$ $L \geq L_{c1}$	$T_u = 18C_u B_s \left[\frac{M_y}{9C_u B_s} + \frac{L^2}{2} + \frac{9}{8} \cdot B_s^2 \right]^{1/2} - (0.75B_s + 0.5L) \quad (5-23c)$	
	$L_{c1} = \left[2.25B_s^2 + \frac{4}{9} \cdot \frac{M_y}{9C_u B_s} \right]^{1/2} + \left[\frac{M_y}{2.25C_u B_s} \right]^{1/2} \quad (5-23d)$	
Long $L \geq L_{c1}$	$T_u = 9C_u B_s \left[(2.25B_s^2 + \frac{4}{9} M_y)^{1/2} - 1.5B_s \right] \quad (5-23e)$	

d. Fixed Head Pile in Cohesionless Soil

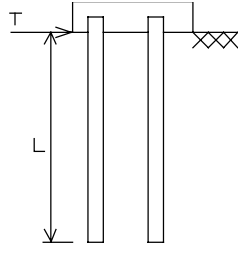
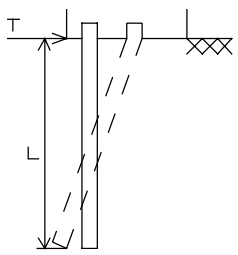
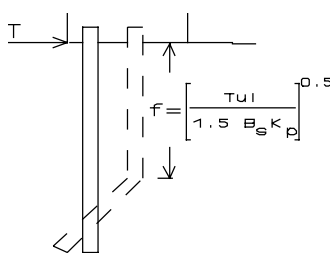
Pile	Equations	Diagram
Short $L \leq L_{cs}$	$T_s = 1.5\gamma B_s K_p L^2 \quad (5-25a)$	
	$L_{cs} = \left[\frac{M_y}{\gamma B_s K_p} \right]^{1/3} \quad (5-25b)$	

TABLE 5-5 (Concluded)

Pile	Equations	Diagram
Inter-mediate $L_{cs} \leq L_{c1}$ $L \geq L_{c1}$	$T_u = \frac{M_y}{L} + 0.5\gamma B_s K_p$ (5-25c)	
	$L_{c1}^3 - \frac{T_{u1}}{0.5\gamma B_s K_p} \cdot L_{c1} + \frac{M_y}{0.5\gamma B_s K_p}$ (5-25d)	
Long $L \geq L_{c1}$	$T_u = \frac{2M_y}{e + \frac{2}{3} \cdot f}$ (5-25e)	

e. Nomenclature

B_s	= diameter of pile shaft, ft
C_u	= undrained shear strength, kips/ft ²
c	= distance from centroid to outer fiber, ft
e	= length of pile above ground surface, ft
$1.5B_s + f$	= distance below ground surface to point of maximum bending moment in cohesive soil, ft
f	= distance below ground surface to point of maximum bending moment in cohesionless soil, ft
f_y	= pile yield strength, ksf
I_p	= pile moment of inertia, ft ⁴
K_p	= Rankine coefficient of passive pressure, $\tan^2(45 + \phi'/2)$
L	= embeded pile length, ft
L_c	= critical length between long and short pile, ft
L_{cs}	= critical length between short and intermediate pile, ft
L_{c1}	= critical length between intermediate and long pile, ft
M_a	= applied bending moment, positive in clockwise direction, kips-ft
M_y	= ultimate resisting bending moment of entire cross-section, kips-ft
T	= lateral load, kips
T_u	= ultimate lateral load, kips
T_{u1}	= ultimate lateral load of long pile in cohesionless soil, kips
Z	= section modulus I_p/c , ft ³
Z_{max}	= maximum section modulus, ft ³
Z_{min}	= minimum section modulus, ft ³
γ	= unit wet weight of soil, kips/ft ³
ϕ'	= effective angle of internal friction of soil, degrees

(1) **Considerations.**

(a) Lateral load failure may occur in short drilled shafts and piles, which behave as rigid members, by soil failure and excessive pile deflection and in long piles by excessive bending moment.

(b) Computation of lateral deflection for different shaft penetrations may be made to determine the depth of penetration at which additional penetration will not significantly decrease the groundline deflection. This depth will be approximately $4\beta_e$ for a soil in which the soil stiffness increases linearly with depth

$$\beta_e = \left[\frac{E_p I_p}{k} \right]^{1/5} \quad (5-26)$$

where

E_p = elastic modulus of shaft or pile, ksf

I_p = moment of inertia of shaft, ft^4

k = constant relating elastic soil modulus with depth, $E_s = kz$
kips/ ft^3

Shafts which carry insignificant axial loads such as those supporting overhead signs can be placed at this minimum depth if their lateral load capacity is acceptable.

(c) Cyclic loads reduce the support provided by the soil, cause gaps to appear near the ground surface adjacent to the shaft, increase the lateral deflection for a given applied lateral load and can reduce the ultimate lateral load capacity because of the loss of soil support.

(d) Refer to ASTM D 3966 for details on conducting lateral load tests.

(2) **Broms' Closed Form Solution.** Broms' method uses the concept of a horizontal coefficient of subgrade reaction and considers short pile failure by flow of soil around the pile and failure of long piles by forming a plastic hinge in the pile. Refer to Broms (1964a), Broms (1964b), Broms (1965), and Reese (1986) for estimating T_u from charts.

(a) Cohesive soil to depth $1.5B_s$ is considered to have negligible resistance because a wedge of soil to depth $1.5B_s$ is assumed to move up and when the pile is deflected.

(b) Iteration is required to determine the ultimate lateral capacity of long piles T_{ul} in cohesionless soil, Table 5-5. Distance f , Table 5-5b and 5-5d, may first be estimated and T_{ul} calculated; then, f is calculated and T_{ul} recalculated as necessary. T_{ul} is independent of length L in long piles.

(3) **Load Transfer Analysis.** The method of solution using load transfer p - y curves is also based on the concept of a coefficient of horizontal subgrade reaction. A fourth-order differential equation is solved using finite differences and load transfer p - y curves.

(a) Numerous p-y relationships are available to estimate appropriate values of soil stiffness for particular soil conditions (Reese 1986). p-y curves developed from local experience and back-calculated from lateral load tests may also be used in program COM624G.

(b) Program COM624G has provided excellent agreement with experimental data for many load test results.

b. **Allowable Lateral Loads.** Estimates of allowable lateral load T_a is best accomplished from results of lateral load-deflection (p-y) analysis using given p-y curves and a computer program such as COM624G. The specified maximum allowable lateral deflection should be used to estimate T_a .

(1) Minimum and maximum values of the expected soil modulus of subgrade reaction should be used to determine a probable range of lateral load capacity. This modulus may be estimated from results of pressuremeter tests using the Menard deformation modulus (Reese 1986), estimates of the elastic soil modulus with depth, or values given in Table 5-6b.

(2) A rough estimate of allowable lateral load T_a may be made by calculating lateral groundline deflection y_o using Equations in Table 5-6,

$$T_a = \frac{y_a}{y_o} \cdot T_u \quad (5-27)$$

where y_a is a specified allowable lateral deflection and T_u is estimated from equations in Table 5-5.

c. **Example Application.** A concrete drilled shaft is to be constructed to support a design lateral load $T_d = 10$ kips. This load will be applied at the ground surface, therefore length above the ground surface $e = 0$. Lateral deflection should be no greater than $y_a = 0.25$ inch. An estimate is required to determine a suitable depth of penetration and diameter to support this lateral load in a clay with cohesion $C_u = 1$ ksf for a soil in which the elastic modulus is assumed to increase linearly with depth. A trial diameter $B_s = 2.5$ ft (30 inches) is selected with 1 percent steel. Yield strength of the steel $f'_{ys} = 60$ ksi and concrete strength $f'_c = 3$ ksi.

(1) **Minimum Penetration Depth.** The minimum penetration depth may be estimated from Equation 5-26 using $E_p I_p$ and k . Table 5-7 illustrates calculation of $E_p I_p$ for a reinforced concrete shaft which is $2.7 \cdot 10^5$ kips-ft². $k = 170$ kips/ft³ from Table 5-6b when the elastic modulus increases linearly with depth. Therefore,

$$\beta_e = \left[\frac{E_p I_p}{k} \right]^{1/5} = \left[\frac{2.7 \cdot 10^5}{170} \right]^{1/5} = 4.37 \text{ ft}$$

The minimum depth of penetration $L = 4\beta_e = 4 \cdot 4.37 = 17.5$ ft. Select $L = 20$ ft.

TABLE 5-6

Estimation of Ultimate Lateral Deflection y_o at the Groundline
(Broms 1964a, Reese 1986)

a. Soil With Modulus of Subgrade Reaction Constant With Depth

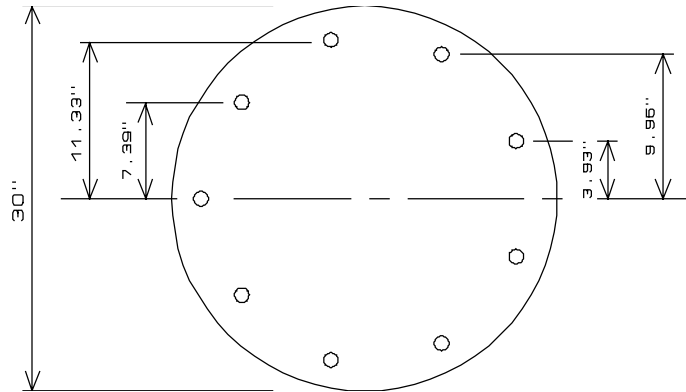
File	Equation	Remarks
Short Free Head $\beta_c L < 1.5$	$y_o = \frac{4T_u (1 + 1.5 \frac{e}{L})}{E_{sl} L}$	$\beta_c = \left[\frac{E_{sl}}{4E_p I_p} \right]^{1/4}$ E_p = pile lateral elastic modulus, ksf I_p = pile moment of inertia, ft ⁴ E_{sl} = modulus of subgrade reaction, ksf
Short Fixed Head $\beta_c L < 0.5$	$y_o = \frac{T_u}{E_{sl} L}$	Terzaghi Recommendations for E_{sl}
Long Free Head $\beta_c L > 1.5$	$y_o = \frac{2T_u \beta_c}{E_{sl}}$	Clay C_u , ksf E_{sl} , ksf
Long Fixed Head $\beta_c L > 1.5$	$y_o = \frac{T_u \beta_c}{E_{sl}}$	Stiff 1 - 2 3 - 6 Very Stiff 2 - 4 6 - 13 Hard > 4 > 13

b. Soil With Modulus of Subgrade Reaction Increasing Linearly With Depth

Equation	Definitions																				
$y_o = F_y \frac{T_u \beta_\ell^3}{E_p I_p}$	$\beta_\ell = \left[\frac{E_p I_p}{k} \right]^{1/5}$ k = constant relating elastic soil modulus with depth, $E_s = kz$, kips/ft ³																				
	Representative Values for k																				
	<table border="1"> <thead> <tr> <th rowspan="2">C_u, kips/ft²</th> <th colspan="2">k, kips/ft³</th> </tr> <tr> <th>Static</th> <th>Cyclic</th> </tr> </thead> <tbody> <tr> <td>0.25 - 0.5</td> <td>50</td> <td>20</td> </tr> <tr> <td>0.50 - 1.0</td> <td>170</td> <td>70</td> </tr> <tr> <td>1.0 - 2.0</td> <td>500</td> <td>200</td> </tr> <tr> <td>2.0 - 4.0</td> <td>1700</td> <td>700</td> </tr> <tr> <td>4.0 - 8.0</td> <td>5000</td> <td>2000</td> </tr> </tbody> </table>	C_u , kips/ft ²	k , kips/ft ³		Static	Cyclic	0.25 - 0.5	50	20	0.50 - 1.0	170	70	1.0 - 2.0	500	200	2.0 - 4.0	1700	700	4.0 - 8.0	5000	2000
C_u , kips/ft ²	k , kips/ft ³																				
	Static	Cyclic																			
0.25 - 0.5	50	20																			
0.50 - 1.0	170	70																			
1.0 - 2.0	500	200																			
2.0 - 4.0	1700	700																			
4.0 - 8.0	5000	2000																			
	Values for F_y																				
	<table border="1"> <thead> <tr> <th>$\frac{L}{\beta_\ell}$</th> <th>F_y</th> </tr> </thead> <tbody> <tr> <td>2</td> <td>1.13</td> </tr> <tr> <td>3</td> <td>1.03</td> </tr> <tr> <td>4</td> <td>0.96</td> </tr> <tr> <td>5</td> <td>0.93</td> </tr> </tbody> </table>	$\frac{L}{\beta_\ell}$	F_y	2	1.13	3	1.03	4	0.96	5	0.93										
$\frac{L}{\beta_\ell}$	F_y																				
2	1.13																				
3	1.03																				
4	0.96																				
5	0.93																				

TABLE 5-7

Example $E_p I_p$ Computation of Drilled Shafts
(After American Concrete Institute Committee 318, 1980)



Cross-section area: 707 in²
 Steel area (1 %): 7.07 in² < 7.11 in² for 9 #8 bars, ASTM 60 grade steel
 ASTM 60 grade steel $f'_{ys} = 60,000$ psi
 Concrete strength $f'_c = 3,000$ psi
 $E_c = 57.5 \cdot (f'_c)^{1/2} : 3149$ kips/in²

Gross moment of inertia:
 $I_g = \pi B_s^4 / 64 = \pi \cdot 30^4 / 64 = 39,760$ in⁴
 $E_{st} = 29,000$ kips/in²
 Area of #8 bar, $A_{st} = 0.79$ in²

Steel moment of inertia about centroid axis, I_{st} :
 $I_{st} = 2 \cdot A_{st} \sum (\text{distance from central axis})^2$
 $= 2 \cdot 0.79 \cdot (11.33^2 + 9.96^2 + 7.39^2 + 3.93^2)$
 $= 470.25$ in⁴

Calculation of $E_p I_p$:
 Using ACI Code Equation 10.8 (approximate)

$$E_p I_p = \frac{E_c I_g}{2.5} = \frac{3149 \cdot 39760}{2.5} = 5 \cdot 10^7 \text{ kips-in}^2$$

Using ACI Code Equation 10.7 (more accurate)

$$\begin{aligned} E_p I_p &= \frac{E_c I_g}{5} + E_{st} I_{st} \\ &= 2.5 \cdot 10^7 + 29000 \cdot 470.25 \\ &= 3.86 \cdot 10^7 \text{ kips-in}^2 \\ &= 2.68 \cdot 10^5 \text{ kips-ft}^2 \end{aligned}$$

(2) **Ultimate Lateral Load.** Broms equations in Table 5-5a for a free head pile in cohesive soil may be used to roughly estimate T_u . The ultimate bending moment resistance M_y using data in Table 5-7 is

$$\begin{aligned} M_y &= 1.3 f_y Z = 1.3 [f'_{ys} Z_{st} + 0.03 f'_c Z_c] \\ &= 1.3 \left[f'_{ys} \sum \frac{I_{st}}{C_{st}} + 0.03 f'_c \frac{2 I_g}{B_s} \right] \\ &= 1.3 \left[60 \cdot 2.079 (11.33 + 9.96 + 7.39 + 3.93) + 0.03 \cdot 3 \frac{2 \cdot 39760}{30} \right] \\ &= 1.3 [94.8 \cdot 32.61 + 238.56] = 4329 \text{ kip-in} \end{aligned}$$

or 360.7 kip-ft. From Table 5-6a

$$\begin{aligned} L_c &= 1.5 B_s + \frac{9}{C_u B_s} + \left[\frac{M_y}{2.25 C_u B_s} \right]^{1/2} \\ &= 1.5 \cdot 2.5 + \frac{9}{1 \cdot 2.5} + \left[\frac{360.7}{2.25 \cdot 1 \cdot 2.5} \right]^{1/2} \\ &= 3.75 + 3.6 + 8.0 = 15.4 \text{ ft} \end{aligned}$$

This shaft with $L = 20$ ft is considered long. From Equation 5-27c, the ultimate lateral load T_u is

$$\begin{aligned} T_u &= 9 C_u B_s \left(\left[(1.5 B_s)^2 + \frac{2 M_y}{9 C_u B_s} \right]^{1/2} - 1.5 B_s \right) \\ &= 9 \cdot 1 \cdot 2.5 \left(\left[(1.5 \cdot 2.5)^2 + \frac{2 \cdot 360.7}{9 \cdot 1 \cdot 2.5} \right]^{1/2} - 1.5 \cdot 2.5 \right) \\ &= 22.5 [14.06 + 32.06]^{1/2} - 3.75 = 68.4 \text{ kips} \end{aligned}$$

(3) **Allowable Lateral Load.** From Table 5-6b, the ultimate lateral deflection y_o is

$$\begin{aligned} y_o &= F_y \frac{T_u B_s^3}{E_p I_p} \\ &= 0.95 \frac{68.4 \cdot 4.4^3}{2.7 \cdot 10^5} \\ &= 0.022 \text{ ft} \end{aligned}$$

or 0.26 inch. On the basis of Equation 5-27 the design displacement will be $(10/68.4) \cdot 0.26$ or 0.04 inch, which is less than the specified allowable deflection $y_a = 0.25$ inch. The trial dimensions are expected to be fully adequate to support the design lateral load of 10 kips. Additional analysis using COM624G should be performed to complete a more economical and reliable design.

5-5. **Capacity of Shaft Groups.** Drilled shafts are often not placed in closely spaced groups because these foundations can be constructed with large diameters and can extend to deep depths. The vertical and lateral load capacities of shaft foundations are often the sum of the individual drilled shafts. The FS for groups should be 3.

a. **Axial Capacity.** The axial capacity of drilled shafts spaced $\geq 8B_s$ will be the sum of the capacities of individual shafts. If drilled shafts are constructed in closely spaced groups where spacing between shafts is $< 8B_s$, then the capacity of the group may be less than the sum of the capacities of the individual shafts. This is because excavation of a hole for a shaft reduces effective stresses against both the sides and bases of shafts already in place. Deep foundations where spacings between individual piles are less than 8 times the shaft width B also cause interaction effects between adjacent shafts from overlapping of stress zones in the soil, Figure 5-13. In situ soil stresses from shaft loads are applied over a much larger area leading to greater settlement and bearing failure at lower total loads.

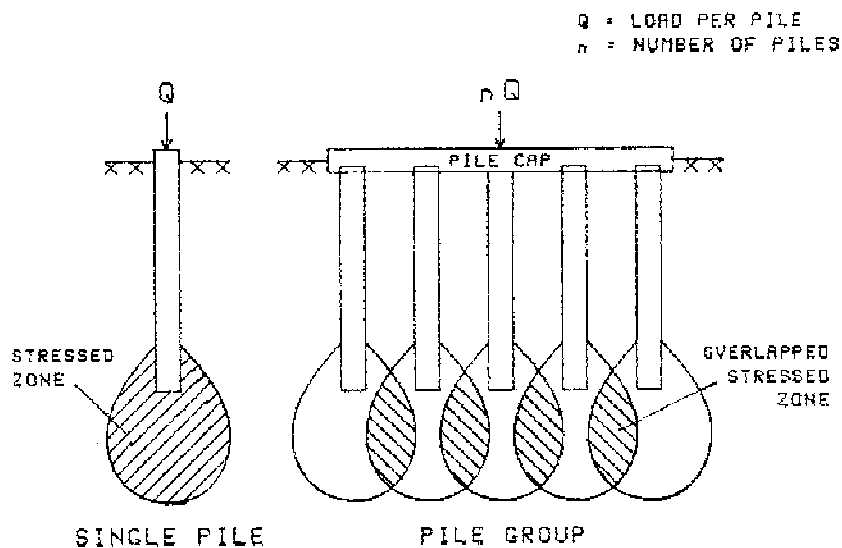


Figure 5-13. Stress zones in soil supporting group

(1) **Cohesive Soil.** Group capacity may be estimated by efficiency and equivalent methods. The efficiency method is recommended when the group cap is isolated from the soil surface, while the equivalent method is recommended when the cap is resting on the soil surface. The equivalent method is useful for spacings $\leq 3B_s$ where B_s is the shaft or pile diameter, Figure 5-14.

(a) Group ultimate capacity by the efficiency method is

where

$$Q_{ug} = n \cdot E_g \cdot Q_u \tag{5-28a}$$

- Q_{ug} = group capacity, kips
- n = number of shafts in the group
- E_g = efficiency
- Q_u = ultimate capacity of the single shaft, kips

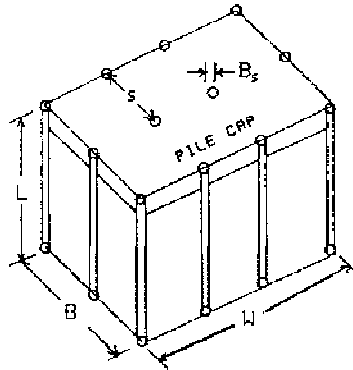


Figure 5-14. Schematic of group

E_g should be > 0.7 for spacings $> 3B_s$ and 1.0 for spacings $> 8B_s$. E_g should vary linearly for spacings between $3B_s$ and $8B_s$. $E_g = 0.7$ for spacings $\leq 2.5B_s$.

(b) Group capacity by the equivalent method is

$$Q_{ug} = 2L(B + W)C_{ua} + 9 \cdot C_{ub} \cdot B \cdot W \quad (5-28b)$$

where

- L = depth of penetration, ft
- W = horizontal length of group, ft
- B = horizontal width of group, ft
- C_{ua} = average undrained shear strength of the cohesive soil in which the group is placed, ksf
- C_{ub} = average undrained shear strength of the cohesive soil below the tip to a depth of $2B$ below the tip, ksf

The presence of locally soft soil should be checked because this soil may cause some shafts to fail.

(c) The ultimate bearing capacity of a group in a strong clay soil overlying weak clay may be estimated by assuming block punching through the weak underlying soil layer. Group capacity may be calculated by Equation 5-28b using the undrained strength C_{ub} of the underlying weak clay. A less conservative solution is provided by (Reese and O'Neill 1988)

$$Q_{ug} = Q_{ug,lower} + \frac{H_b}{10B} [Q_{ug,upper} - Q_{ug,lower}] \leq Q_{ug,upper} \quad (5-29)$$

where

- $Q_{ug,lower}$ = bearing capacity if base at top of lower (weak) soil, kips
- $Q_{ug,upper}$ = bearing capacity in the upper soil if the softer lower soil soil were not present, kips
- H_b = vertical distance from the base of the shafts in the group to the top of the weak layer, ft
- B = least width of group, ft

(2) **Cohesionless Soil.** During construction of drilled shafts in cohesionless soil, stress relief may be more severe than in cohesive soils because cohesionless soils do not support negative pore pressures as well as cohesive soils. Negative pore pressures generated during excavation in cohesive soils tend to keep effective stresses higher than in cohesionless soil.

(a) The efficiency Equation 5-28a is usually recommended.

(b) Equation 5-29 can be used to estimate ultimate bearing capacity of a group in a strong cohesionless soil overlying a weak cohesive layer.

b. **Lateral Load Capacity.** Response of groups to lateral load requires lateral and axial load soil-structure interaction analysis with assistance of a finite element computer program.

(1) **Widely Spaced Drilled Shafts.** Shafts spaced $> 7B_s$ or far enough apart that stress transfer is minimal and loading is by shear, the ultimate lateral load of the group T_{ug} is the sum of individual shafts. The capacity of each shaft may be estimated by methodology in 5-4.

(2) **Closely Spaced Drilled Shafts.** The solution of ultimate lateral load capacity of closely spaced shafts in a group requires analysis of a nonlinear soil-shaft system

$$T_{ug} = \sum_{j=1}^n T_{uj} \quad (5-30)$$

where

T_{uj} = ultimate lateral load capacity of shaft j , kips
 n = number of shafts in the group

Refer to Poulos (1971a, Poulos (1971b), and Reese (1986) for detailed solution of the lateral load capacity of each shaft by the Poulos-Focht-Koch method.

(3) **Group Behavior as a Single Drilled Shaft.** A pile group may be simulated as a single shaft with diameter C_g/π where C_g is the circumference given as the minimum length of a line that can enclose the group. The moment of inertia of the group is $n \cdot I_p$ where I_p is the moment of inertia of a single shaft. Program COM624G may be used to evaluate lateral load-deflection behavior of the simulated single shaft for given soil conditions. Comparison of results between the Poulos-Focht-Koch and simulated single pile methods was found to be good (Reese 1986).

Section II. Driven Piles

5-6. **Effects of Pile Driving.** Driving piles disturbs and substantially remolds soil. Driving radially compresses cohesive soils and increases the relative density of cohesionless soils near the pile.

a. **Cohesive Soil.** Soil disturbance around piles driven into soft or normally consolidated clays is within one pile diameter. Driving into saturated stiff clays closes fissures and causes complete loss of stress history near the pile (Vesic 1969).

(1) **Driving in Saturated Clay.** Soil disturbance and radial compression increase pore water pressures that temporarily reduce the soil shear strength and pile load capacity. Pore pressures decrease with time after driving and lead to an increase in shear strength and pile load capacity. This effect is soil freeze.

(2) **Driving in Unsaturated Clay.** Driving in unsaturated clay does not generate high pore pressures and probably will not lead to soil freeze.

b. **Cohesionless Soil.** The load capacity of cohesionless soil depends strongly on relative density. Driving increases relative density and lateral displacement within a zone around the pile of one to two pile diameters. Large displacement piles such as closed end pipe piles cause larger increases in relative density than small displacement piles such as H-piles. The increase in bearing capacity can therefore be greater with large displacement piles.

(1) **Driving in Dense Sand and Gravel.** Driving in dense sand and gravel can decrease pore pressures from soil dilation and temporarily increase soil shear strength and pile load capacity. Shear strength can increase substantially and may exceed the capacity of pile driving equipment to further drive the piles into the soil. Pore pressures increase after driving and cause the shear strength to decrease and reduce the pile load capacity. This effect is soil relaxation.

(2) **Driving in Saturated Cohesionless Silts.** Driving in saturated cohesionless silts increases pore pressures and can temporarily reduce the soil shear strength and pile load capacity. Pore pressures dissipate after driving and lead to an increase in shear strength and pile load capacity. This effect is soil freeze as described in cohesive soil, but can occur more quickly than in cohesive soil because permeability is greater in silts.

5-7. **Vertical Capacity of Single Driven Piles.** The vertical capacity of driven piles may be estimated using Equations 5-1 similar to drilled shafts

$$Q_u \approx Q_{bu} + Q_{su} - W_p \quad (5-1a)$$

$$Q_u \approx q_{bu}A_b + \sum_{i=1}^n Q_{sui} - W_p \quad (5-1b)$$

where

- Q_u = ultimate bearing capacity, kips
- Q_{bu} = ultimate end bearing resistance, kips
- Q_{su} = ultimate skin friction, kips
- q_{bu} = unit ultimate end bearing resistance, ksf
- A_b = area of tip or base, ft²
- n = number of pile elements
- Q_{sui} = ultimate skin friction of pile element i , ksf
- W_p = pile weight, $\approx A_b \cdot L \cdot \gamma_p$ without enlarged base, kips
- L = pile length, ft
- γ_p = pile density, kips/ft³

In addition, a wave equation analysis should be performed to estimate the driving forces to prevent pile damage during driving, to estimate the total driving resistance that will be encountered by the pile to assist in determining the

required capability of the driving equipment and to establish pile driving criteria. Refer to program GRLWEAP (Goble Rausche Likins and Associates, Inc. 1988) for details of wave equation analysis. Pile driving formulas are also recommended to quickly estimate the ultimate bearing capacity.

a. **End Bearing Capacity.** End bearing capacity may be estimated by

$$Q_{bu} = c \cdot N_{cp} \cdot \zeta_{cp} + \sigma'_L \cdot N_{qp} \cdot \zeta_{qp} + \frac{B_b}{2} \cdot \gamma'_b \cdot N_{\gamma p} \cdot \zeta_{\gamma p} \quad (5-2a)$$

where

- c = cohesion of soil beneath the tip, ksf
- σ'_L = effective soil vertical overburden pressure at pile base
 $\approx \gamma' \cdot L$, ksf
- γ'_L = effective wet unit weight of soil along shaft length L,
kips/ft³
- B_b = base diameter, ft
- γ'_b = effective wet unit weight of soil beneath base, kips/ft³
- N_{cp}, N_{qp}, N_{γp} = pile bearing capacity factors of cohesion, surcharge, and
wedge components
- ζ_{cp} , ζ_{qp} , $\zeta_{\gamma p}$ = pile soil and geometry correction factors of cohesion,
surcharge, and wedge components

Equation 5-2a may be simplified for driven piles by eliminating the N_{γp} term

$$Q_{bu} = c \cdot N_{cp} \cdot \zeta_{cp} + \sigma'_L \cdot (N_{qp} - 1) \cdot \zeta_{qp} \quad (5-2b)$$

or

$$Q_{bu} = c \cdot N_{cp} \cdot \zeta_{cp} + \sigma'_L \cdot N_{qp} \cdot \zeta_{qp} \quad (5-2c)$$

Equations 5-2b and 5-2c also adjust for pile weight W_p assuming $\gamma_p \approx \gamma'_L$. Equation 5-2c is usually used because omitting the "1" is usually negligible. Bearing capacity does not increase without limit with increasing depth. Refer to Figure 5-3 to determine the critical depth L_c below which effective stress remains constant using the Meyerhof and Nordlund methods.

(1) **Cohesive Soil.** The shear strength of cohesive soil is $c = C_u$, the undrained strength, and the effective friction angle $\phi' = 0$. Equation 5-2a leads to

$$Q_{bu} = N_{cp} \cdot C_u = 9 \cdot C_u \quad (5-2d)$$

where shape factor $\zeta_{cp} = 1$ and $N_{cp} = 9$. Undrained shear strength C_u is estimated by methods in Chapter 3 and may be taken as the average shear strength within $2B_b$ beneath the tip of the pile.

(2) **Cohesionless Soil.** Meyerhof, Nordlund, and in situ methods described below and Hanson, Vesic, and general shear methods described in Section I are recommended for solution of ultimate end bearing capacity using Equations 5-2. Several of these methods should be used for each design problem to provide a reasonable range of probable bearing capacity if calculations indicate a significant difference between methods.

(a) Meyerhof Method. Figure 5-15 illustrates the bearing capacity factors to be used with Equation 5-2b (Meyerhof 1976). The range between "low" and "high" factors in Figure 5-15 should account for soil conditions such as loose or dense sands, overconsolidation ratio of clays, and soils with different degrees of compressibility. The correction factors ζ_{cp} and ζ_{qp} in Equation 5-2b are unity. N_{cp} and N_{qp} are estimated as follows:

Evaluate the critical depth ratio $R_c = L_c/B$ from the given friction angle ϕ' using Figure 5-3. Then calculate the critical depth $L_c = R_c \cdot B$ where B = pile diameter or width.

1. If $\phi' < 30^\circ$ and $L > L_c/2$, then use $N_{cp,high}$ and $N_{qp,high}$ directly from curves of Figure 5-15

2. If $\phi' < 30^\circ$ and $L < L_c/2$, then from Figure 5-15

$$N_{cp} = N_{cp,low} + (N_{cp,high} - N_{cp,low}) \frac{2L}{L_c} \quad (5-31a)$$

$$N_{qp} = N_{qp,low} + (N_{qp,high} - N_{qp,low}) \frac{2L}{L_c} \quad (5-31b)$$

If $\phi' \geq 30^\circ$, evaluate the bearing depth ratio $R_b = L/B$, locate the intersection of R_b and ϕ' in Figure 5-15, then estimate by interpolation N_{cb} and N_{qp} , respectively.

3. If $R_b > R_c$, check to be sure that $q_{bu} \leq q_l =$ the limiting stress. The limiting stress is given by

$$q_l = N_{qp} \cdot \tan \phi' \quad (5-31c)$$

where q_l is in units of ksf.

Refer to Vanikar (1986) for further applications using the Meyerhof method.

(b) Nordlund Method. This semi-empirical method considers the shape of the pile taper and the influence of soil displacement on skin friction. Equations for calculating ultimate capacity are based on load test results that include timber, steel H, pipe, monotube, and Raymond steptaper piles. Ultimate capacity is determined by, Figure 5-16

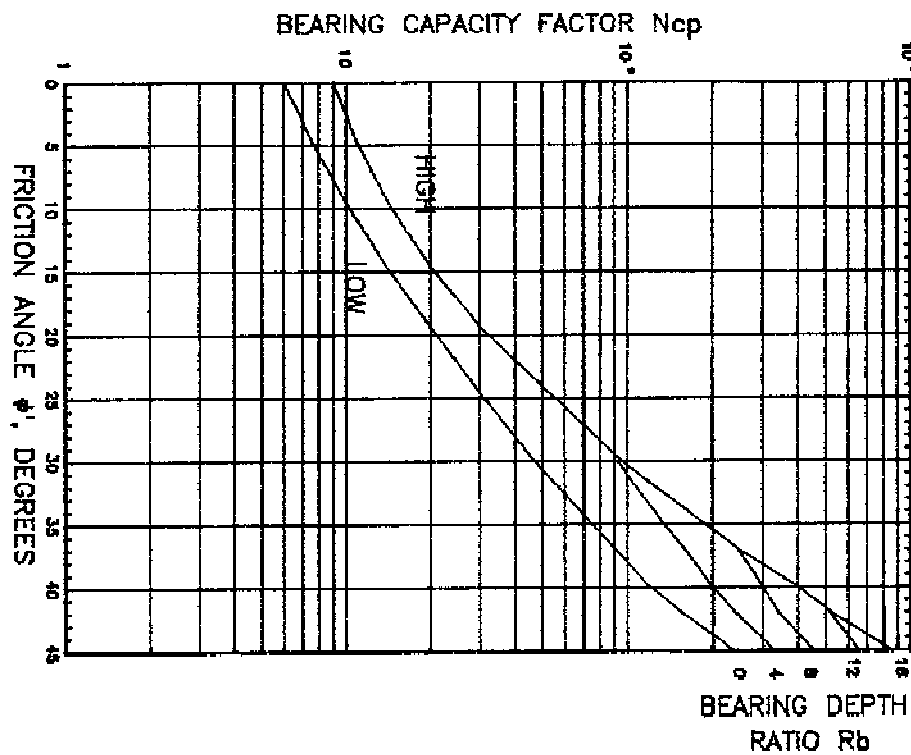
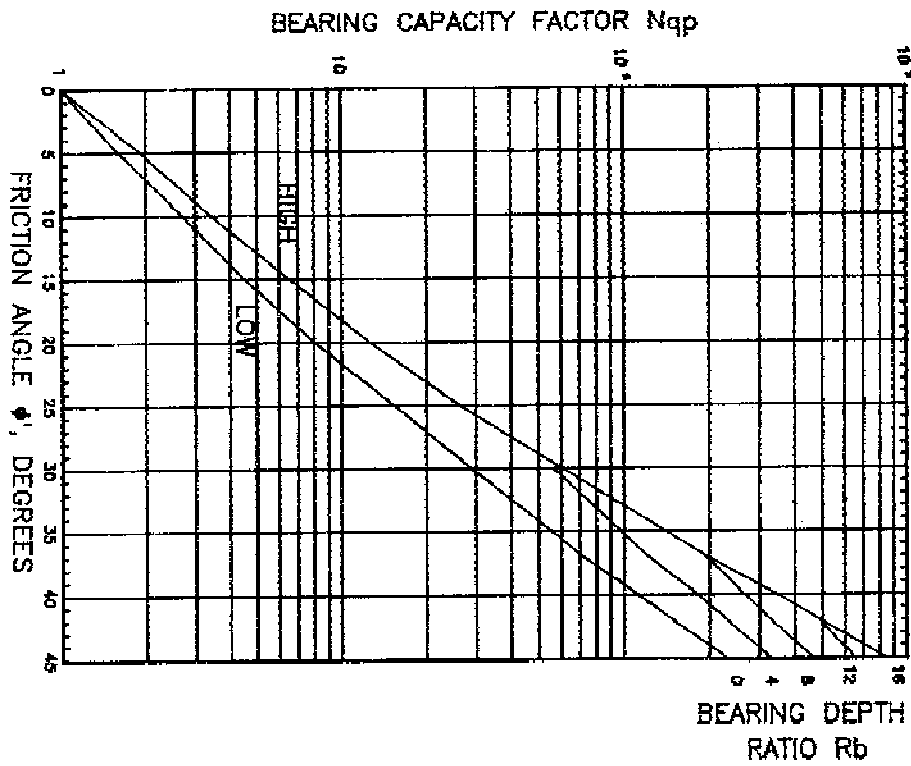


Figure 5-15. Bearing capacity factors for Meyerhof method (Data from Meyerhof 1976)

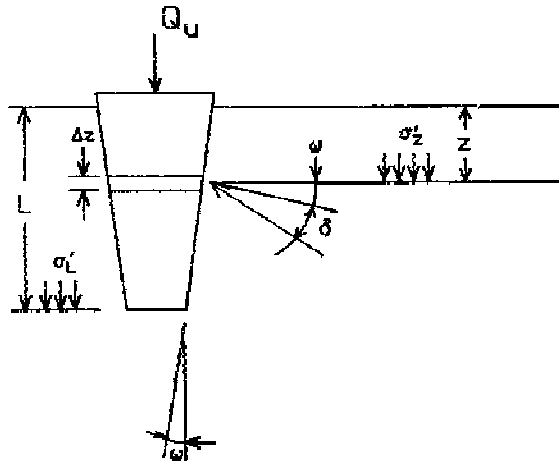


Figure 5-16. Illustration of input parameters for Nordlund's equation.

$$Q_u = \alpha_f N_{qp} A_b \sigma'_L + \sum_{z=0}^{z=L} KC_f \sigma'_z \frac{\sin(\delta + \omega)}{\cos \omega} C_z \Delta L \quad (5-32a)$$

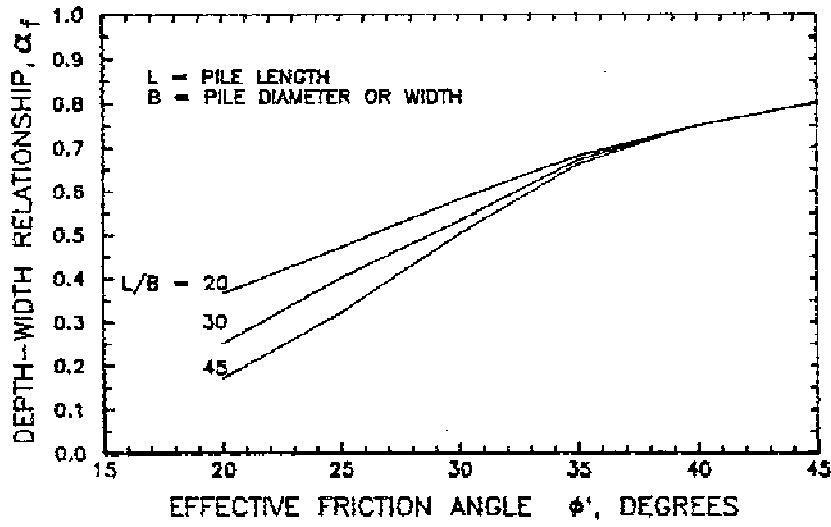
where

- α_f = dimensionless pile depth-width relationship factor
- A_b = pile point area, ft^2
- σ'_L = effective overburden pressure at pile point, ksf
- K = coefficient of lateral earth pressure at depth z
- C_f = correction factor for K when $\delta \neq \phi'$
- ϕ' = effective soil friction angle, degrees
- δ = friction angle between pile and soil
- ω = angle of pile taper from vertical
- σ'_z = effective overburden pressure at the center of depth increment ΔL , $0 < z \leq L$, ksf
- C_z = pile perimeter at depth z , ft
- ΔL = pile increment, ft
- L = length of pile, ft

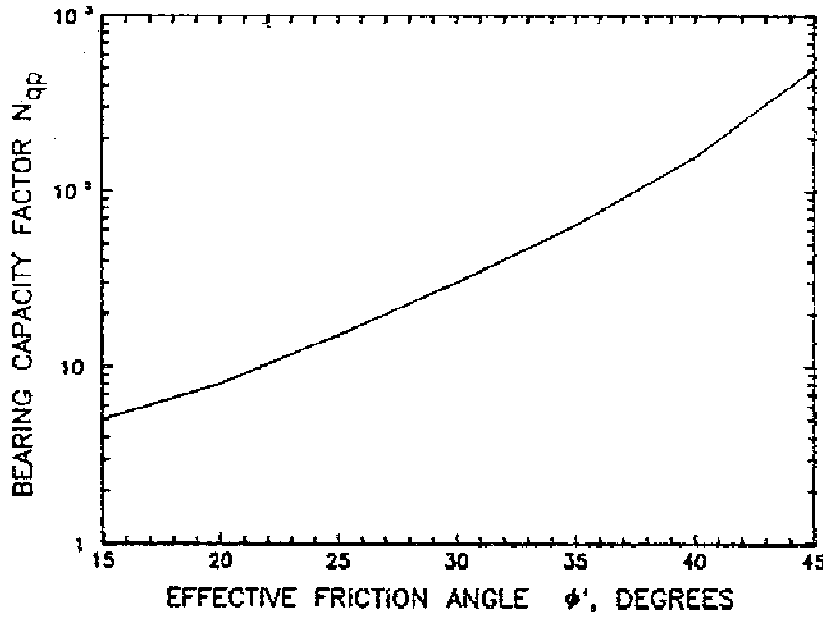
ϕ' may be estimated from Table 3-1. Point resistance $q_{bu} = \alpha_f N_{qp} \sigma'_L A_p$ should not exceed $q_u A_p$ where q_u is given by Equation 5-31c. α_f and N_{qp} may be found from Figure 5-17, K from Figure 5-18, δ from Figure 5-19 for a given ϕ' and C_f may be found from Figure 5-20. Equation 5-32a for a pile of uniform cross-section ($\omega = 0$) and length L driven in a homogeneous soil with a single friction angle ϕ and single effective unit weight is

$$Q_u = \alpha_f N_{qp} A \sigma'_m + KC_f \sigma'_m \sin \delta C_s L \quad (5-32b)$$

where A is the pile cross-section area, C_s is the pile perimeter and σ'_m is the mean effective vertical stress between the ground surface and pile tip, ksf . Table 5-8 provides a procedure for using the Nordlund method (Data from Vanikar 1986).

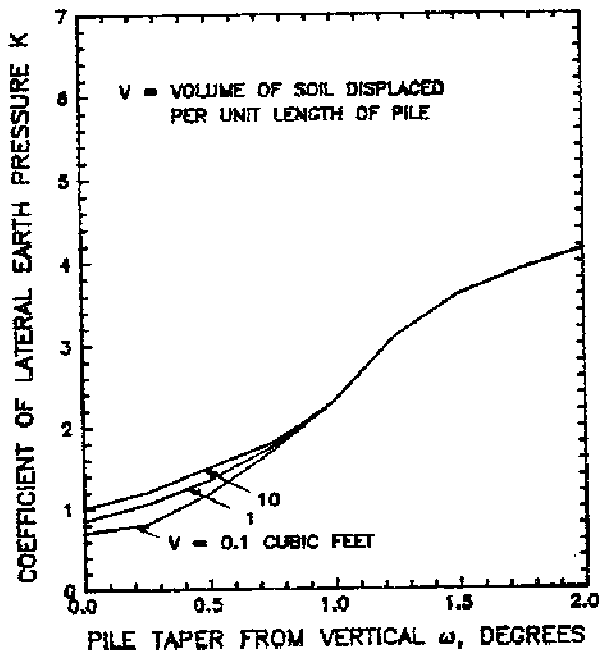


a. α_f

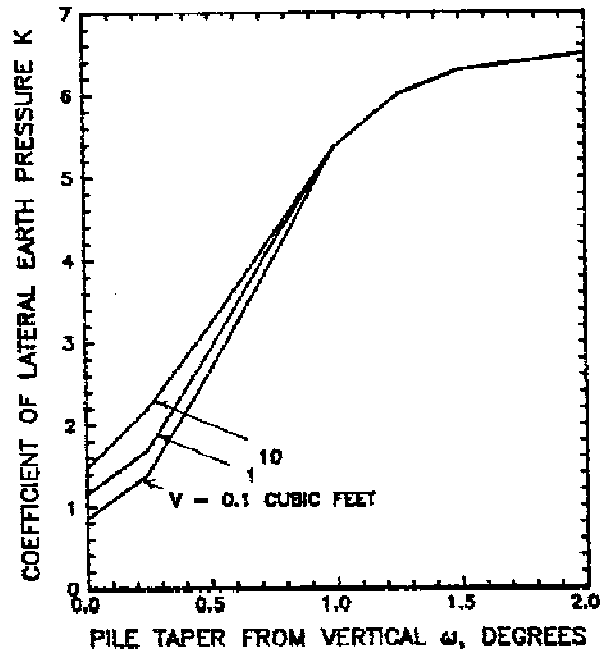


b. N_{qp}

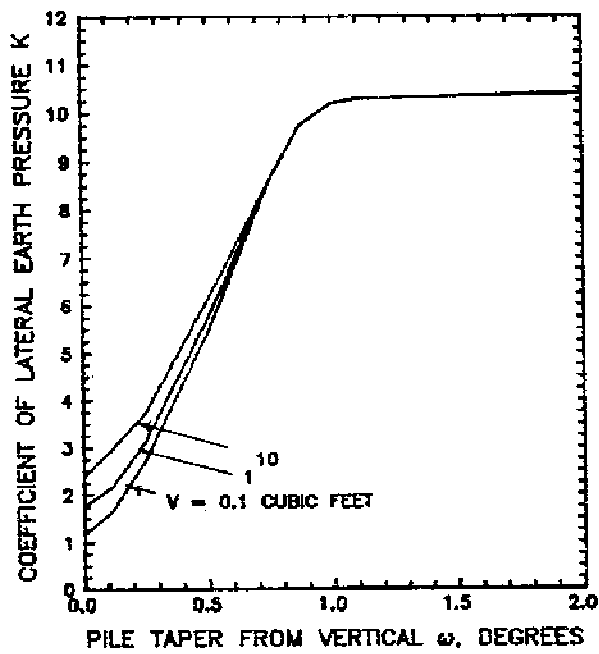
Figure 5-17. Coefficient α_f and bearing capacity factor N_{qp} for the Nordlund method (Data from Vanikar 1986)



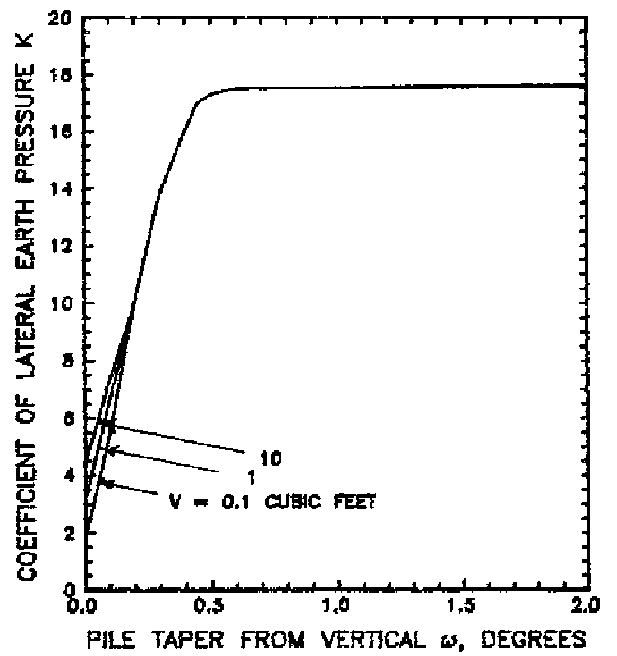
a. $\phi' = 25^\circ$



b. $\phi' = 30^\circ$



c. $\phi' = 35^\circ$



d. $\phi' = 40^\circ$

Figure 5-18. Coefficient K for various friction angles ϕ' and pile taper ω for Nordlund method (Data from Vanikar 1986)

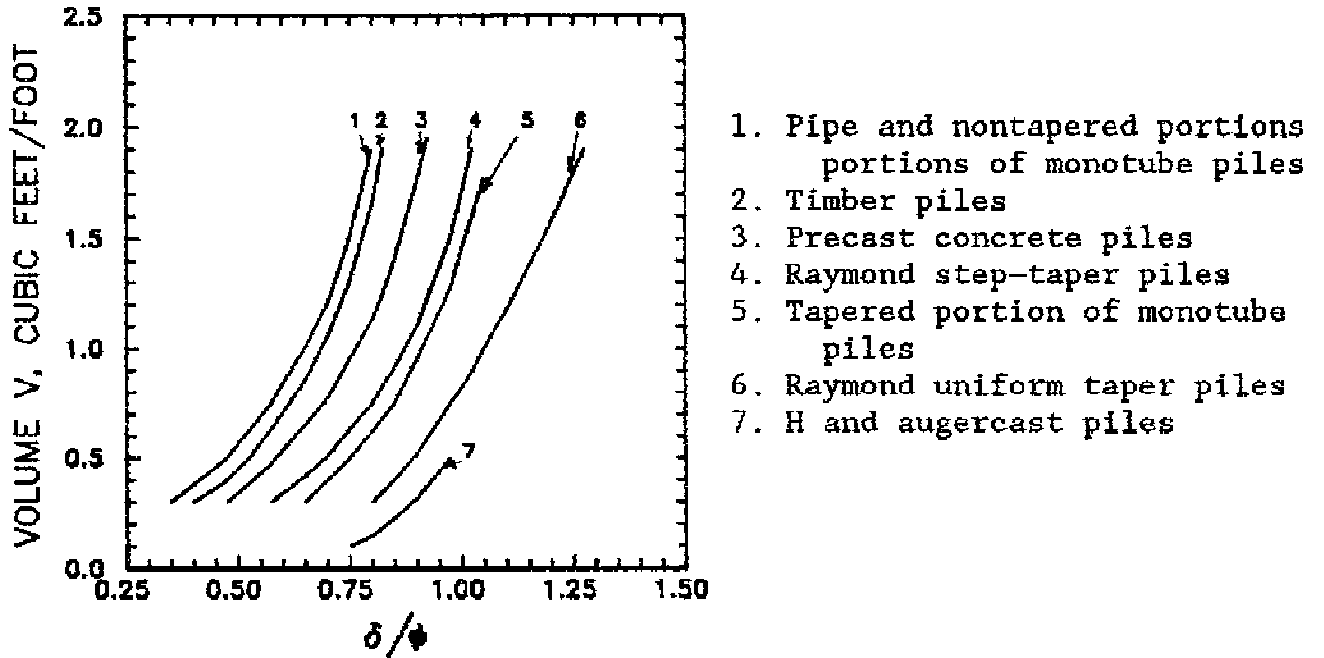


Figure 5-19. Ratio δ/ϕ for given displacement volume V
(Data from Vanikar 1986)

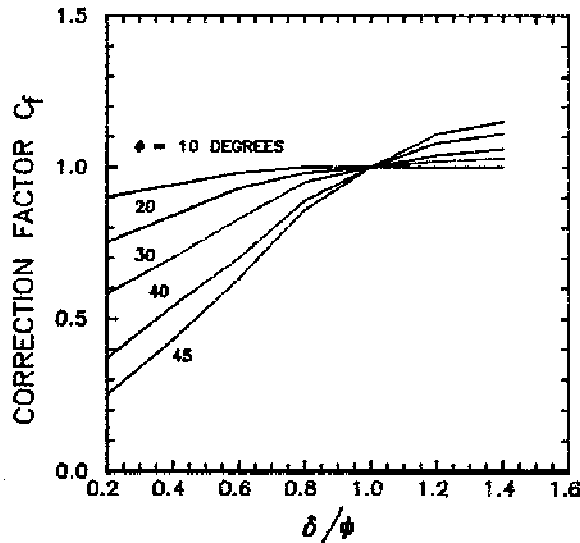


Figure 5-20. Correction factor C_f when $\delta \neq \phi$
(Data from Vanikar 1986)

TABLE 5-8

Procedure for the Nordlund Method

Step	Procedure
<u>a. End Bearing Capacity</u>	
1	Determine friction angle ϕ' from in situ test results using Tables 3-1 and 3-2 for each soil layer. $\phi = \phi'$
2	Determine α_f using ϕ for the soil layer in which the tip is embedded and the pile L/B ratio from Figure 5-17a
3	Determine N_{qp} using ϕ for the soil layer in which the tip is embedded from Figure 5-17b
4	Determine effective overburden pressure at the pile tip, σ'_L
5	Determine the pile point area, A_b
6	Determine end bearing resistance pressure $q_{bu} = \alpha_f N_{qp} \sigma'_L$. Check $q_{bu} \leq q_\ell = N_{qp} \tan \phi$ of Equation 5-31c. Calculate end bearing capacity $Q_{bu} = q_{bu} A_b \leq q_\ell A_b$. N_{qp} used in Equation 5-31c should be determined by Meyerhof's method using Figure 5-15
<u>b. Skin Friction Capacity</u>	
7	Compute volume of soil displaced per unit length of pile
8	Compute coefficient of lateral earth pressure K for ϕ' and ω using Figure 5-18. Use linear interpolation
9	Determine δ/ϕ for the given pile and volume of displaced soil V from Figure 5-19. Calculate δ for friction angle ϕ
10	Determine correction factor C_f from Figure 5-20 for ϕ and the δ/ϕ ratio
11	Calculate the average effective overburden pressure σ'_z of each soil layer
12	Calculate pile perimeter at center of each soil layer C_z
13	Calculate the skin friction capacity of the pile in each soil layer i from
	$Q_{sui} = KC_f \sigma'_z \frac{\sin(\delta + \omega)}{\cos \omega} C_z \Delta L$
	Add Q_{sui} of each soil layer to obtain Q_{su} , $Q_{su} = \sum Q_{sui}$ of each layer
14	Compute ultimate total capacity, $Q_u = Q_{bu} + Q_{su}$

(3) **Field Estimates From In Situ Soil Tests.** The ultimate end bearing capacity of soils may be estimated from field tests if laboratory soil or other data are not available.

(a) SPT Meyerhof Method. End bearing capacity may be estimated from penetration resistance data of the SPT by (Meyerhof 1976)

$$q_{bu} = 0.8 \cdot N_{SPT} \cdot \frac{L_b}{B} < 8 \cdot N_{SPT}, \quad \frac{L_b}{B} \geq 10 \quad (5-33)$$

where N_{SPT} is the average uncorrected blow count within $8B_b$ above and $3B_b$ below the pile tip. L_b is the depth of penetration of the pile tip into the bearing stratum. q_{bu} is in units of ksf.

(b) CPT Meyerhof method. End bearing capacity may be estimated from cone penetration resistance data by (Meyerhof 1976)

$$q_{bu} = \frac{q_c \cdot L_b}{10 \cdot B} < q_\ell \quad (5-34)$$

based on numerous load tests of piles driven to a firm cohesionless stratum not underlain by a weak deposit. q_ℓ is the limiting static point resistance given approximately by Equation 5-31c. N_{qp} should be estimated by the Meyerhof method, Table 4-3. q_{bu} and q_ℓ are in units of ksf.

(c) CPT B & G method. End bearing capacity may also be estimated from cone penetration resistance data by (Bustamante and Gianceselli 1983)

$$q_{bu} = k_c \cdot q_c \quad (5-35)$$

where

k_c = point correlation factor, Table 5-9

q_c = average cone point resistance within $1.5B_b$ below the pile point, ksf

B_b = base diameter, ft

TABLE 5-9

Point Correlation Factor k_c (Bustamante and Gianceselli 1983)

Soil	k_c	
	Driven Pile	Drilled Shaft
Clay - Silt	0.600	0.375
Sand - Gravel	0.375	0.150
Chalk	0.400	0.200

(d) CPT 1978 FHWA-Schmertmann method (modified). End bearing capacity may be estimated by (Schmertmann 1978)

$$q_{bu} = \frac{q_{c1} + q_{c2}}{2} \quad (5-36)$$

where q_{c1} and q_{c2} are unit cone resistances determined by the procedure described in Figure 5-21. For example, q_{c1} calculated over the minimum path is as follows:

$$q_{c1} = \frac{180+170+170+170+170}{5} = 172 \text{ ksf}$$

q_{c2} over the minimum path is as follows:

$$q_{c2} = \frac{120+150+160+160+160+160+160+160}{8} = 153.75 \text{ ksf}$$

From Equation 5-36, $q_{bu} = (172 + 153.75)/2 = 162.9 \text{ ksf}$.

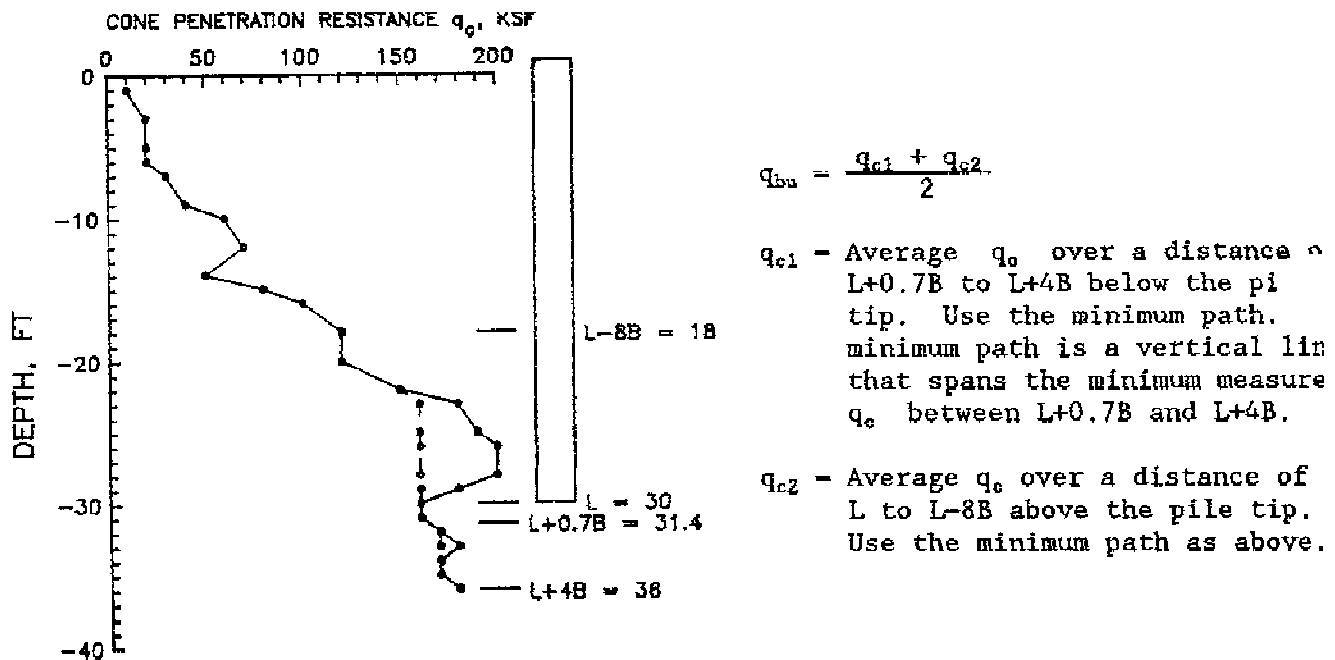


Figure 5-21. Estimating pile tip capacity from CPT data
(Data from Schmertmann 1978)

(4) **Scale Effects.** Ultimate end bearing capacity q_{bu} tends to be less for larger diameter driven piles and drilled shafts than that indicated by Equations 5-33 or 5-34 or Equation 5-2b using Equations 5-31 to estimate N_{cp} or N_{qp} (Meyerhof 1983). Skin friction is independent of scale effects.

(a) Sands. The reduction in end bearing capacity has been related with a reduction of the effective angle of internal friction ϕ' with larger diameter deep foundations. End bearing capacity q_{bu} from Equation 5-2 should be multiplied by a reduction factor R_{bs} (Meyerhof 1983)

$$R_{bs} = \left[\frac{B + 1.64}{2B} \right]^m \leq 1 \quad (5-37a)$$

for $B > 1.64$ ft. The exponent $m = 1$ for loose sand, 2 for medium dense sand, and 3 for dense sand.

(b) Clays. The reduction factor R_{bc} appears related to soil structure and fissures. For driven piles in stiff fissured clay, R_{bc} is given by Equation 5-37a where $m = 1$. For bored piles

$$R_{bc} = \left[\frac{B + 3.3}{2B + 3.3} \right] \leq 1 \quad (5-37b)$$

for B from 0 to 5.75 ft.

b. **Skin Resistance Capacity.** The maximum skin resistance that may be mobilized along an element of pile length ΔL may be estimated by

$$Q_{sui} = A_{si} \cdot f_{si} \quad (5-9)$$

where

A_{si} = area of pile element i , $C_{si} \cdot \Delta L$, ft^2
 C_{si} = shaft circumference at pile element i , ft
 ΔL = length of pile element, ft
 f_{si} = skin friction at pile element i , ksf

(1) **Cohesive Soil.**

(a) Alpha method. The skin friction of a length of pile element may be estimated by

$$f_{si} = \alpha_a \cdot C_u \quad (5-10)$$

where

α_a = adhesion factor
 C_u = undrained shear strength, ksf

Local experience with existing soils and load test results should be used to estimate appropriate α_a . Estimates of α_a may be made from Table 5-10 in the absence of load test data and for preliminary design.

(b) Lambda Method. This semi-empirical method is based on numerous load test data of driven pipe piles embedded in clay assuming that end bearing capacity was evaluated from Equation 5-2a using $N_{cp} = 9$ and $\zeta_{cp} = 1$ (Vijayvergiya and Focht 1972). The N_{qp} and N_{yp} terms are not used. Skin friction is

$$f_{si} = \lambda \cdot (\sigma'_m + 2C_{um}) \quad (5-38a)$$

where

λ = correlation factor, Figure 5-22
 σ'_m = mean effective vertical stress between the ground surface and pile tip, ksf
 C_{um} = mean undrained shear strength along the pile length, ksf

TABLE 5-10

Adhesion Factors for Driven Piles in Cohesive Soil
 (Data from Tomlinson 1980)

Length/Width Ratio $\frac{L}{B}$	Undrained Shear Strength C_u , ksf	Adhesion Factor α_a
< 20	< 3	$1.2 - 0.3C_u$
	> 3	0.25
> 20	0.0 - 1.5	1.0
	1.5 - 4.0	$1.5 - 0.4C_u$
	> 4	0.3

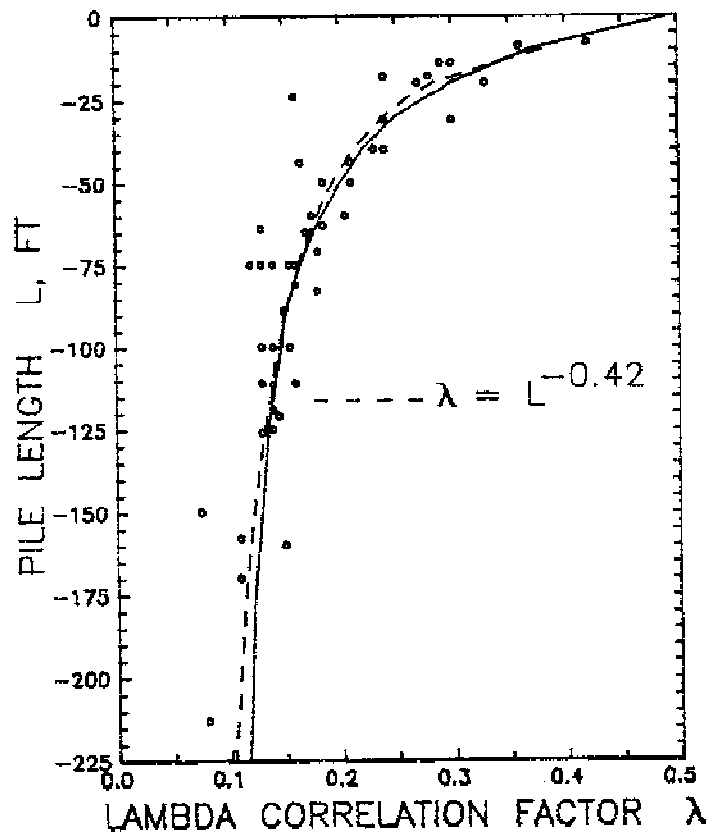


Figure 5-22. Lambda correlation factor
 (Data from Vijayvergiya and Focht 1972)

λ may also be given approximately by

$$\lambda = L^{-0.42} \quad L \geq 10FT \quad (5-38b)$$

where L is the pile length, ft.

(2) **Cohesionless Soil.** The soil-shaft skin friction may be estimated using effective stresses

$$f_{si} = \beta_f \cdot \sigma'_i \quad (5-12a)$$

$$\beta_f = K \cdot \tan \delta_a \quad (5-12b)$$

where

β_f = lateral earth pressure and friction angle factor

K = lateral earth pressure coefficient

δ_a = soil-shaft effective friction angle, $\leq \phi'$, deg

σ'_i = effective vertical stress in soil in pile element i , ksf

Cohesion c is taken as zero.

(a) Figure 5-5 indicates appropriate values of β_f as a function of the effective friction angle ϕ' of the soil prior to installation of the deep foundation.

(b) The effective vertical stress σ'_i approaches a limiting stress at the critical depth L_c , then remains constant below L_c . L_c may be estimated from Figure 5-3.

(c) The Nordlund method in Table 5-8b provides an alternative method of estimating skin resistance.

(3) **CPT Field Estimate.** The skin friction f_{si} may be estimated from the measured cone resistance q_c for the piles described in Table 5-2b using the curves given in Figure 5-6 for clay and silt, sand and gravel, and chalk (Bustamante and Gianceselli 1983).

c. **Ultimate Capacity From Wave Equation Analysis.** Estimates of total bearing capacity may be performed using computer program GRLWEAP (Goble Rausche Likins and Associates, Inc. 1988). The analysis uses wave propagation theory to calculate the force pulse transmitted along the longitudinal pile axis caused by impact of the ram, Figure 5-23. The force pulse travels at a constant velocity depending on the pile material and this pulse is attenuated by the soil frictional resistance along the embedded length of the pile. The pile penetrates into the soil when the force pulse reaching the pile tip exceeds the ultimate soil resistance at the pile tip Q_{ub} . Program GRLWEAP and user's manual are licensed to the Waterways Experiment Station and it is available to the US Army Corps of Engineers.

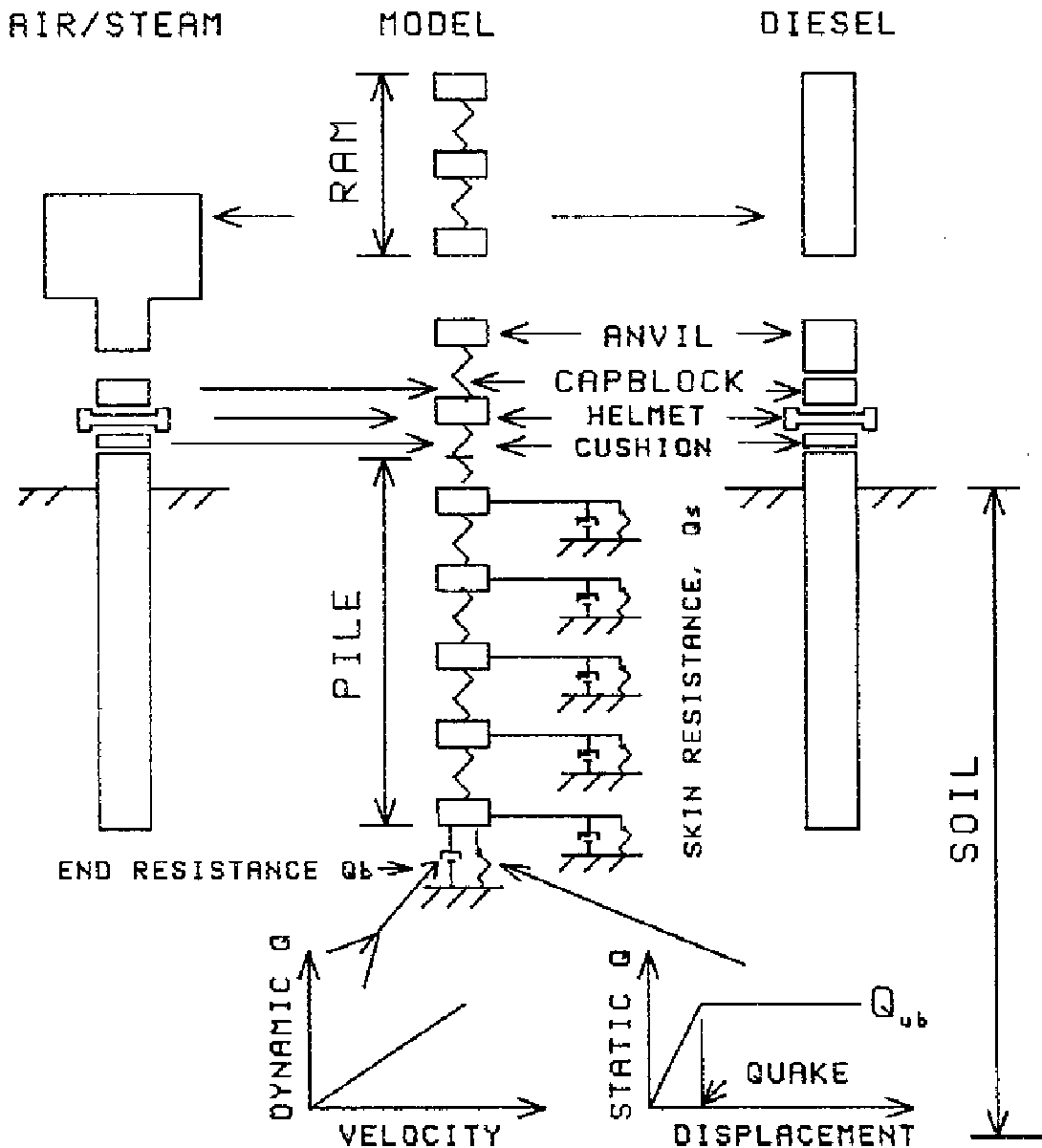


Figure 5-23. Schematic of wave equation model

(1) **Description.** The pile driving and soil system consists of a series of elements supported by linear elastic springs and dashpots which have assumed parameters, Figure 5-23. Characteristics of commonly used pile hammers and piles are available in the program data files driving systems. Input parameters include the dynamic damping constants for each dashpot, usually in units of seconds/inch, ultimate soil resistance Q_u in kips and quake in fractions of an inch for each spring. Each dashpot and spring represent a soil element. The quake of the pile is its displacement at Q_{ub} . Input data for Q_{ub} , quake, and ultimate skin resistance of each element Q_{sui} are usually assumed. Actual load distribution data are

normally not available and require results of instrumented load tests. Standard values are available in the user's manual for soil input parameters.

(2) **Analysis.** The wave equation analysis provides a relationship between the pile capacity and the driving resistance in blows per inch (or blows per foot if needed). This relationship can be developed for different pile lengths and then used in the field when the pile has been driven sufficiently to develop the required capacity. The wave equation can also be used to develop relationships between driving stresses in the pile and penetration resistance for different combinations of piles and pile driving equipment.

(3) **Application.** The wave equation analysis is used to select the most suitable driving equipment to ensure that the piles can develop the required capacity and select the minimum pile section required to prevent overstressing the pile during driving.

(4) **Calibration.** Calculations from program GRLWEAP may be calibrated with results of dynamic load tests using pile driving analyzer (PDA) equipment. The force and velocity versus time curves calculated from GRLWEAP are adjusted to agree with the force and velocity versus time curves measured by the PDA during pile driving or during a high strain test. A high strain causes a force at the pile tip sufficient to exceed the ultimate soil resistance Q_{ub} . Drilled shafts may be analyzed with the PDA during a high strain test where heavy loads are dropped by a crane on the head of the shaft.

(5) **Factors of Safety.** In general, pile capacity calculated by GRLWEAP should be divided by a factor of safety $FS = 3$ to estimate allowable capacity or $FS = 2.5$ if calibrated with results of dynamic load tests. If load tests are performed, $FS = 2$ can be used with GRLWEAP.

(6) **Restriking.** Soils subject to freeze or relaxation could invalidate a wave equation analysis; therefore, installed piles should be tested by restriking while using PDA equipment after a minimum waiting period following installation such as 1 day or more as given in the specifications.

d. **Pile Driving Formulas.** Pile driving formulas, Table 5-11, although not as good as wave equation analysis, can provide useful, simple estimates of ultimate pile capacity Q_u and they can be obtained quickly. The allowable bearing capacity can be estimated from Equations 1-2 using FS in Table 5-11. Two or more of these methods should be used to provide a probable range of Q_u .

e. **Example Application.** A steel circular 1.5-ft diameter closed end pipe pile is to be driven 30 ft through a 2-layer soil of clay and fine uniform sand, Figure 5-7. The water table is 15 ft below ground surface at the clay-sand interface. The pile will be filled with concrete grout with density $\gamma_{conc} = 150$ lbs/ft³. Design load $Q_d = 100$ kips.

(1) **Soil Parameters.**

(a) The mean effective vertical stress in the sand layer adjacent to the embedded pile σ'_s and at the pile tip σ'_L is limited to 1.8 ksf for the Meyerhof and Nordlund methods. Otherwise, σ'_L is 2.4 ksf from Equation 5-13b.

TABLE 5-11

File Driving Formulas

Method	Equation for Ultimate Bearing Capacity Q_u , kips	Factor of Safety
Gates	$27(E_h E_r)^{1/2} (1 - \log_{10} S)$	3
Pacific Coast Uniform Building Code	$\frac{12E_h E_r C_{p1}}{S + C_{p2}}$, $C_{p1} = \frac{W_r + c_p W_p}{W_r + W_p}$, $C_{p2} = \frac{Q_u L}{AE_p}$ $c_p = 0.25$ for steel piles; $= 0.10$ for other piles Initially assume $C_{p2} = 0$ and compute Q_u ; reduce Q_u by 25 percent, compute C_{p2} , then recompute Q_u ; compute a new C_{p2} , compute Q_u until Q_u used = Q_u computed	4
Danish	$\frac{12E_h E_r}{S + C_d}$, $C_d = \left[\frac{144E_h E_r L}{2AE_p} \right]^{1/2}$, inches	3 - 6
Engineering News Record	Drop Hammers: $\frac{12W_r h}{S + 1.0}$ Other Hammers: $\frac{24E_r}{S + 0.1}$	6 6

Nomenclature:

- A = area of pile cross-section, ft²
- E_h = hammer efficiency
- E_p = pile modulus of elasticity, ksf
- E_r = manufacturer's hammer-energy rating (or $W_r h$), kips-ft
- h = height of hammer fall, ft
- L = pile length, inches
- S = average penetration in inches per blow for the last 5 to 10 blows for drop hammers and 10 to 20 blows for other hammers
- W_r = weight of striking parts of ram, kips
- W_p = weight of pile including pile cap, driving shoe, capblock and anvil for double-acting steam hammers, kips

(b) The average undrained shear strength of the upper clay layer is $C_u = 2$ ksf. The friction angle of the lower sand layer is estimated at $\phi' = 36$ deg. Cone penetration test results shown in Figure 5-21 indicate an average cone tip resistance $q_c = 40$ ksf in the clay and 160 ksf in the sand.

(2) **End Bearing Capacity.** A suitable estimate of end bearing capacity q_{bu} for the pile tip in the sand may be evaluated from the various methods for cohesionless soil as described below.

(a) Meyerhof Method. From Figure 5-3, $R_c = 10$ and $L_c = R_c \cdot B = 10 \cdot 1.5$ or 15 ft for $\phi' = 36$ deg. N_{qp} from Figure 5-15 is 170 for $R_b = L/B = 15/1.5 = 10$. From Equation 5-2c with limiting pressure q_ℓ from Equation 5-31c

$$\begin{aligned} q_{bu} &= \sigma'_L \cdot N_{qp} \leq N_{qp} \cdot \tan\phi' \quad \text{if } L > L_c \\ \sigma'_L \cdot N_{qp} &= 1.8 \cdot 170 = 306 \text{ ksf} \\ N_{qp} \cdot \tan\phi' &= 170 \cdot \tan 36 = 123.5 \text{ ksf} \\ q_{bu} &\leq q_\ell, \text{ therefore } q_{bu} = 123.5 \text{ ksf} \end{aligned}$$

(b) Nordlund Method. The procedure in Table 5-8a may be used to estimate end bearing capacity.

$$\begin{aligned} \alpha_f &= 0.67 \text{ for } \phi' = 36 \text{ deg from Figure 5-17a} \\ N_{qp} &= 80 \text{ for } \phi' = 36 \text{ deg from Figure 5-17b} \\ \sigma'_L &= 1.8 \text{ ksf} \\ q_{up} &= \alpha_f N_{qp} \sigma'_L = 0.67 \cdot 80 \cdot 1.8 = 96.5 \text{ ksf} \\ q_\ell &= N_{qp} \tan\phi' = 170 \cdot \tan 36 = 123.5 \text{ ksf where } N_{qp} \text{ is from Figure 5-15.} \end{aligned}$$

$$\text{Therefore, } q_{bu} = 96.5 \text{ ksf} \leq q_\ell$$

(c) Hansen Method. From Table 4-5 (or calculated from Table 4-4) $N_{qp} = 37.75$ and $N_{\gamma p} = 40.05$ for $\phi' = 36$ deg. From Table 4-5,

$$\begin{aligned} \zeta_{qs} &= 1 + \tan\phi = 1 + \tan 36 = 1.727 \\ \zeta_{qd} &= 1 + 2 \tan\phi (1 - \sin\phi)^2 \cdot \tan^{-1}(L_{sand}/B) \\ &= 1 + 2 \tan 36 (1 - \sin 36)^2 \cdot \tan^{-1}(15/1.5) \cdot \pi/180 \\ &= 1 + 2 \cdot 0.727 (1 - 0.588)^2 \cdot 1.471 = 1.363 \\ \zeta_{qp} &= \zeta_{qs} \cdot \zeta_{qd} = 1.727 \cdot 1.363 = 2.354 \\ \zeta_{\gamma s} &= 1 - 0.4 = 0.6 \\ \zeta_{\gamma d} &= 1.00 \\ \zeta_{\gamma p} &= \zeta_{\gamma s} \cdot \zeta_{\gamma d} = 0.6 \cdot 1.00 = 0.6 \end{aligned}$$

From Equation 5-2a

$$\begin{aligned} q_{bu} &= \sigma'_L \cdot N_L \cdot \zeta_{qp} + (B_b/2) \cdot \gamma'_s \cdot N_{\gamma p} \cdot \zeta_{\gamma p} \\ &= 2.4 \cdot 37.75 \cdot 2.354 + (1.5/2) \cdot 0.04 \cdot 40.05 \cdot 0.6 \\ &= 213.3 + 0.7 = 214 \text{ ksf} \end{aligned}$$

The $N_{\gamma p}$ term is negligible and could have been omitted.

(d) Vesic Method. The reduced rigidity index from Equation 5-5c is

$$I_{rr} = \frac{I_r}{1 + \epsilon_v \cdot I_r} = \frac{57.3}{1 + 0.006 \cdot 57.3} = 42.6$$

where

$$\text{(Equation 5-5e): } \epsilon_v = \frac{1 - 2 \cdot \mu_s}{2(1 - \mu_s)} \cdot \frac{\sigma'_L}{G_s} = \frac{1 - 2 \cdot 0.3}{2(1 - 0.3)} \cdot \frac{2.4}{100} = 0.006$$

$$\text{(Equation 5-5d): } I_r = \frac{G_s}{\sigma'_L \cdot \tan\phi'} = \frac{100}{2.4 \cdot \tan 36} = 57.3$$

From Equation 5-5b

$$N_{qp} = \frac{3}{3 - \sin\phi'} \cdot e^{\frac{(90-\phi')\pi}{180} \tan\phi'} \cdot \tan^2 \left[45 + \frac{\phi'}{2} \right] \cdot I_{rr} \frac{4 \sin\phi'}{3(1 + \sin\phi')}$$

$$N_{qp} = \frac{3}{3 - \sin 36} \cdot e^{\frac{(90-36)\pi}{180} \tan 36} \cdot \tan^2 \left[45 + \frac{36}{2} \right] \cdot I_{rr} \frac{4 \sin 36}{3(1 + \sin 36)}$$

$$N_{qp} = \frac{3}{3 - 0.588} e^{0.685} \cdot 3.852 \cdot 42.6^{0.494}$$

$$N_{qp} = 1.244 \cdot 1.984 \cdot 3.852 \cdot 6.382 = 60.7$$

The shape factor from Equation 5-6a is

$$\zeta_{qp} = \frac{1 + 2K_o}{3} = \frac{1 + 2 \cdot 0.42}{3} = 0.61$$

where K_o was evaluated using Equation 5-6c. From Equation 5-2c,

$$q_{bu} = \sigma'_L \cdot N_{qp} \cdot \zeta_{qp} = 2.4 \cdot 60.7 \cdot 0.61 = 88.9 \text{ ksf}$$

(e) General Shear Method. From Equation 5-8

$$N_{qp} = \frac{e^{\frac{270-\phi'}{180} \cdot \pi \tan\phi'}}{2 \cos^2 \left[45 + \frac{\phi'}{2} \right]} = \frac{e^{\frac{270-36}{180} \cdot \pi \tan 36}}{2 \cos^2 \left[45 + \frac{\phi'}{2} \right]} = \frac{e^{1.3\pi \cdot 0.727}}{2 \cdot 0.206}$$

$$N_{qp} = \frac{19.475}{0.412} = 47.24$$

The shape factor $\zeta_{qp} = 1.00$ when using Equation 5-8. From Equation 5-2c,

$$q_{bu} = \sigma'_L \cdot N_{qp} \cdot \zeta_{qp} = 2.4 \cdot 47.24 \cdot 1.00 = 113.4 \text{ ksf}$$

(f) CPT Meyerhof Method. From Equation 5-34

$$q_{bu} = \frac{q_c \cdot L_{sand}}{10 \cdot B} < q_\ell$$

where $q_\ell = N_{qp} \cdot \tan\phi'$ ksf. Substituting the parameters into Equation 5-34

$$q_{bu} = \frac{160}{10} \cdot \frac{15}{1.5} = 160 \text{ ksf}$$

The limiting q_ℓ is 123.5 ksf, therefore $q_{bu} = 123.5 \text{ ksf}$

(g) CPT B & G. From Equation 5-35

$$q_{bu} = k_c \cdot q_c$$

where $k_c = 0.375$ from Table 5-9. $q_{bu} = 0.375 \cdot 160 = 60 \text{ ksf}$.

(h) CPT FHWA & Schmertmann. The data in Figure 5-21 can be used with this method to give $q_{bu} = 162.9$ ksf as in the example illustrating this method in paragraph 5-7a.

(i) Comparison of Methods. A comparison of methods is shown as follows:

Method	q_{bu} , ksf
Meyerhof	124
Nordlund	97
Hansen	214
Vesic	89
General Shear	113
CPT Meyerhof	124
CPT B & G	60
CPT FHWA & Schmertmann	163

These calculations indicate q_{bu} from 60 to 214 ksf. Discarding the highest (Hansen) and lowest (CPT B & G) values gives an average $q_{bu} = 118$ ksf. Scale effects of Equations 5-37 are not significant because $B < 1.64$ ft.

(2) **Skin Friction Capacity.** A suitable estimate of skin friction f_s from the soil-shaft interface may be evaluated for both the clay and sand as illustrated below.

(a) Cohesive Soil. The average skin friction using the Alpha method from Equation 5-10 is

$$f_s = \alpha_a \cdot C_u = 0.6 \cdot 2 = 1.2 \text{ ksf}$$

where $\alpha_a = 1.2 - 0.3C_u = 0.6$ from Table 5-11 and $L/B < 20$. The average skin friction using the Lambda method from Equation 5-38a and using $L = 15$ ft for the penetration of the pile only in the clay is

$$f_s = \lambda (\sigma'_m + 2C_{um}) = 0.32 (0.9 + 2 \cdot 2) = 1.57 \text{ ksf}$$

where

$$\lambda = L^{-0.42} = 15^{-0.42} = 0.32 \text{ from Equation 5-38b}$$

$$\sigma'_m = \frac{D_c}{2} \cdot \gamma'_{clay} = \frac{15}{2} \cdot 0.12 = 0.9 \text{ ksf}$$

A reasonable average value of skin friction is 1.4 ksf for the clay.

(b) Cohesionless Soil. The average skin friction from Equation 5-12a using σ'_s limited to 1.8 ksf is

$$f_s = \beta_f \cdot \sigma'_s = 0.96 \cdot 1.8 = 1.7 \text{ ksf}$$

EM 1110-1-1905
30 Oct 92

where β_f is found from Figure 5-5 using $\phi' = 36$ deg. The Nordlund method of Table 5-8b provides an alternative estimate

$$\begin{aligned} V &= \pi \cdot (1.5^2/2) \cdot 1 = 1.77 \text{ ft}^3/\text{ft} \\ K &= 2.1 \text{ from Figure 5-18 for } \omega = 0 \text{ deg} \\ \delta/\phi &= 0.78 \text{ for } V = 1.77 \text{ and pile type 1 from Figure 5-19} \\ \delta &= 0.78 \cdot 36 = 28 \text{ deg} \\ C_f &= 0.91 \text{ for } \delta/\phi = 0.78 \text{ and } \phi = 36 \text{ deg from Figure 5-20} \\ \sigma'_z &= 1.8 \text{ ksf limiting stress} \\ C_z &= \pi \cdot B_s = \pi \cdot 1.5 = 4.71 \text{ ft} \\ Q_{sz} &= KC_f \sigma'_z \sin \delta \cdot C_z \Delta z = 2.1 \cdot 0.91 \cdot 1.8 \cdot \sin 28 \cdot 4.71 \cdot 15 = 114 \text{ kips} \\ f_s &= Q_{sz} / (C_z \Delta z) = 1.6 \text{ ksf} \end{aligned}$$

Skin friction for the sand is about 1.6 ksf.

(c) CPT Field Estimate. The driven pile is described as "steel" from Table 5-2b. Curve 1 of Clay and Silt, Figure 5-6a, and curve 1 of Sand and Gravel, Figure 5-6b, should be used. From these figures, f_s of the clay is 0.7 ksf and f_s of the sand is 0.7 ksf.

(d) Comparison of Methods. Skin friction varies from 0.7 to 1.4 ksf for the clay and 0.7 to 1.6 ksf for the sand. Skin friction is taken as 1.0 ksf in the clay and 1 ksf in the sand.

(3) **Ultimate Total Capacity.** The total bearing capacity from Equation 5-1a is

$$Q_u = Q_{bu} + Q_{su} - W_p$$

where

$$W_p = \frac{\pi B^2}{4} \cdot L \cdot \gamma_{\text{conc}} = \frac{\pi \cdot 1.5^2}{4} \cdot 30 \cdot \frac{150}{1000} = 8 \text{ kips for the pile weight}$$

(a) Q_{bu} may be found from Equation 5-1b

$$Q_{bu} = A_b \cdot q_{bu} = 1.77 \cdot 118 = 209 \text{ kips}$$

where $A_b =$ area of the base, $\pi B^2/4 = \pi \cdot 1.5^2/4 = 1.77 \text{ ft}^2$.

(b) Q_{su} may be found from Equation 5-1b and 5-9

$$Q_{su} = \sum_{i=1}^n Q_{sui} = C_s \cdot \Delta L \sum_{i=1}^2 f_{si}$$

where $C_s = \pi B$. Therefore,

$$\begin{aligned} Q_{su} &= \pi B \cdot (L_{\text{sand}} f_s + L_{\text{clay}} f_s) \\ &= \pi \cdot 1.5 \cdot 15 (1.0 + 1.0) = 141 \text{ kips} \end{aligned}$$

(c) Inserting end bearing and skin resistance bearing capacity values into Equation 5-1a,

$$Q_u = 209 + 141 - 8 = 342 \text{ kips}$$

The minimum and maximum values of q_{bu} and f_s calculated above could be used to obtain a range of Q_u if desired.

(4) **Allowable Bearing Capacity.** The allowable bearing capacity from Equation 1-2b using $FS = 3$ is

$$Q_a = \frac{Q_u}{FS} = \frac{337}{3} = 112 \text{ kips}$$

5-8. **Lateral Load Capacity of Single Piles.** Evaluation of lateral load capacity is treated similarly to that for single drilled shafts in 5-4. Lateral load capacity may be determined by load tests, by analytical methods such as Broms' equations or p-y curves and by arbitrary values. Most piles are placed in groups where group capacity controls performance.

a. Load Tests. Lateral load tests are economically justified for large projects and may be performed as described in ASTM D 3966.

b. Analytical Methods.

(1) Program COM624G using p-y curves are recommended for complicated soil conditions.

(2) Broms' equations in Table 5-5 can give useful estimates of ultimate lateral loads for many cases.

c. Arbitrary Values.

(1) Table 5-12 provides allowable lateral loads for piles.

(2) Piles can sustain transient horizontal loads up to 10 percent of the allowable vertical load without considering design features.

5-9. **Capacity of Pile Groups.** Driven piles are normally placed in groups with spacings less than 8 times the pile diameter or width $8B_p$ and joined at the ground surface by a concrete slab referred to as a pile cap. The capacity of the pile group can be greater than the sum of the capacities of the individual piles because driving compacts the soil and can increase skin friction and end bearing capacity. FS for pile groups should be 3.

a. Axial Capacity. Deep foundations where spacings between individual piles are less than $8B_p$ cause interaction effects between adjacent piles from overlapping of stress zones in the soil, Figure 5-13. In situ soil stresses from pile loads are applied over a much larger area leading to greater settlement and bearing failure at lower total loads.

TABLE 5-12

Recommendations for Allowable Lateral Pile Loads (Data from Vanikar 1986)

Pile	Allowable Deflection, in.	Allowable Lateral Load, kips			Reference
Timber		10			New York State Department of Transportation 1977
Concrete		15			
Steel		20			
All	0.375	2			New York City Building Code 1968
All	0.25	1 (soft clays)			Teng
Timber	0.25	9			Feagin
Timber	0.50	14			"
Concrete	0.25	12			"
Concrete	0.50	17			"
		Medium sand	Fine sand	Medium clay	McNulty
12 inch Timber (free)	0.25	1.5	1.5	1.5	
12 inch Timber (fixed)	0.25	5.0	4.5	4.0	
16 inch Concrete	0.25	7.0	5.5	5.0	

(1) **Optimum Spacing.** Piles in a group should be spaced so that the bearing capacity of the group \geq sum of the individual piles. Pile spacings should not be less than $2.5B_s$. The optimum pile spacing is 3 to $3.5B_s$ (Vesic 1977) or greater than $0.02L + 2.5B_s$ where L is the pile length in feet (Canadian Geotechnical Society 1985).

(2) **Cohesive Soils.** Group capacity may be estimated by efficiency and equivalent methods similar for drilled shafts as described in paragraph 5-5a.

(3) **Cohesionless Soil.** Group capacity should be taken as the sum of the individual piles.

b. **Lateral Load Capacity.** Response of pile groups to lateral load requires lateral and axial load soil-structure interaction analysis with assistance of a finite element computer program.

(1) **Widely Spaced Piles.** Where piles are spaced $> 7B_s$ or far enough apart that stress transfer is minimal and loading is by shear, the ultimate lateral load of the group T_{ug} is the sum of individual piles. The capacity of each pile may be estimated by methodology in 5-4.

(2) **Closely Spaced Piles.** The solution of ultimate lateral load capacity of closely spaced pile groups require analysis of a nonlinear soil-pile system. Refer to Poulos (1971a), Poulos (1971b), and Reese (1986) for detailed solution of the lateral load capacity of each pile by the Poulos-Focht-Koch method.

(3) **Group Behavior as a Single Pile.** A pile group may be simulated as a single pile with diameter C_g/π where C_g is the pile circumference given as the minimum length of a line that can enclose the group of piles. The moment of inertia of the pile group is $n \cdot I_p$ where I_p is the moment of inertia of a single pile. Program COM624G may be used to evaluate lateral load-deflection behavior of the simulated single pile for given soil conditions. A comparison of results between the Poulos-Focht-Koch and simulated single pile methods was found to be good (Reese 1986).

c. **Computer Assisted Analysis.** Computer programs are available from the Waterways Experiment Station to assist in analysis and design of pile groups. Refer to EM 1110-2-2906 for further guidance on the analysis of pile groups.

(1) **Program CPGA.** Pile Group Analysis computer program CPGA is a stiffness analysis in three-dimensions assuming linear elastic pile-soil interaction and a rigid pile cap (Hartman et al 1989). Program CPGA uses matrix methods to incorporate position and batter of piles and piles of different sizes and materials. Computer program CPGG displays the geometry and results of program CPGA (Jaeger, Jobst, and Martin 1988).

(2) **Program CPGC.** Pile Group Concrete computer program CPGC develops the interaction diagrams and data required to investigate the structural capacity of prestressed concrete piles (Strom, Abraham, and Jones 1990).